# Journal Pre-proof


Distinguishing mode of action of compounds inducing craniofacial malformations in zebrafish embryos to support dose-response modeling in combined exposures

Harm J. Heusinkveld, Willem G. Schoonen, Hennie M. Hodemaekers, Anandita Nugraha, Jan-Jaap Sirks, Vivianne Veenma, Carina Sujan, Jeroen L.A. Pennings, Paul F. Wackers, Luca Palazzolo, Ivano Eberini, Emiel Rorije, Leo T.M. van der Ven

PII: S0890-6238(20)30155-6

DOI: https://doi.org/10.1016/j.reprotox.2020.06.002

Reference: RTX 7988

To appear in: *Reproductive Toxicology*

Received Date: 22 November 2019

Revised Date: 26 May 2020

Accepted Date: 1 June 2020

Please cite this article as: Heusinkveld HJ, Schoonen WG, Hodemaekers HM, Nugraha A, Sirks J-Jaap, Veenma V, Sujan C, Pennings JLA, Wackers PF, Palazzolo L, Eberini I, Rorije E, der Ven LTMv, Distinguishing mode of action of compounds inducing craniofacial malformations in zebrafish embryos to support dose-response modeling in combined exposures, *Reproductive Toxicology* (2020), doi: https://doi.org/10.1016/j.reprotox.2020.06.002

# Distinguishing mode of action of compounds inducing craniofacial malformations in zebrafish embryos to support dose-response modeling in combined exposures

Harm J. Heusinkveld[1*], Willem G. Schoonen[2], Hennie M. Hodemaekers[1], Ananditya Nugraha[1], Jan-Jaap Sirks[1], Vivianne Veenma[1], Carina Sujan[1], Jeroen L.A. Pennings[1], Paul F. Wackers[1], Luca Palazzolo[3], Ivano Eberini[4], Emiel Rorije[2], Leo T.M. van der Ven[1]

[1]Department for Innovative Testing Strategies, Centre for Health Protection, National Institute for Public Health and the Environment (RIVM), Bilthoven, the Netherlands
[2]Centre for Safety of Substances and Products, RIVM
[3]Dipartimento di Scienze Farmacologiche e Biomolecolari, Università degli Studi di Milano, Milano, Italy
[4]Dipartimento di Scienze Farmacologiche e Biomolecolari & DSCR, Università degli Studi di Milano, Milano, Italy

*Corresponding author; harm.heusinkveld@rivm.nl

**Graphical abstract**

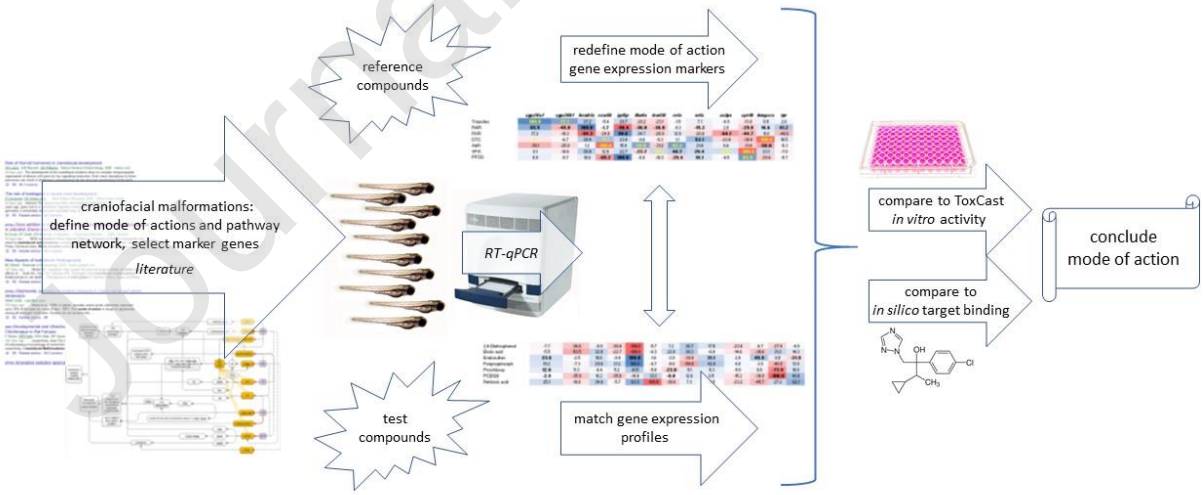

**Highlights**

- Discernable gene expression profiles for MOAs of reference compounds
- GE profiles of unknown compounds can be matched with reference profiles
- MOAs were supported by ToxCast in vitro assays and by molecular docking
- qPCR proved a valuable tool for identification of compound MOAs
- Distinction of MOAs supports modeling of combined exposures

**Abstract**

Knowledge on mode-of-action (MOA) is required to understand toxicological effects of compounds, notably in the context of risk assessment of mixtures. Such information is generally scarce, and often complicated by the existence of multiple MOAs per compound. Here, MOAs related to developmental craniofacial malformations were derived from literature, and assembled in a MOA network. A selection of gene expression markers was based on these MOAs. Next, these markers were verified by qPCR in zebrafish embryos, after exposure to reference compounds. These were: triazoles for inhibition of retinoic acid (RA) metabolism, AM580 and CD3254 for selective activation of respectively RA-receptor (RAR) and retinoid-X-receptor (RXR), dithiocarbamates for inhibition of lysyl oxidase, TCDD for activation of the aryl-hydrocarbon-receptor (AhR), VPA for inhibition of histone deacetylase (HDAC), and PFOS for activation of peroxisome proliferator-activated receptor-alpha (PPARα). Next, marker gene profiles for these reference compounds were used to map the profiles of test compounds to known MOAs. In this way, 2,4-dinitrophenol matched with the TCDD and RAR profiles, boric acid with RAR, endosulfan with PFOS, fenpropimorph with dithiocarbamates, PCB126 with AhR, and RA with triazoles and RAR profiles. Prochloraz showed no match. Activities of these compounds in ToxCast assays, and *in silico* analysis of binding affinity to the respective targets showed limited concordance with the marker gene expression profiles, but still confirmed the complex MOA profiles of reference and test compounds. Ultimately, this approach could be used to support modeling of mixture effects based on upfront knowledge of (dis)similarity of MOAs.

List of Abbreviations

AhR – Aryl hydrocarbon receptor

CAG – Cumulative assessment group (group of chemicals inducing the same effect)

CED20 - Critical effect dose 20%

Cyp26 – Cytochrome P450 26 / Human retinoic acid 4-hydroxylase

Cyp51 - 14α-Sterol demethylase

EFSA – European Food Safety Authority

EGF – Epidermal growth factor

HDAC – Histone deacetylase

hpf – hours post fertilization

HPT-axis – hypothalamus-pituitary-thyroid axis

MOA – Mode of action

MOE – Molecular Operating Environment

PFOS - Heptadecafluoro-1-octanesulfonic acid

PPARα – Peroxisome proliferator-activated receptor alpha

qPCR – quantitative polymerase chain reaction

RA – Retinoic acid

RAR – Retinoic acid receptor

RXR – Retinoid-X-receptor

TCDD - 2,3,7,8-Tetrachlorodibenzo-p-dioxin

TGFbeta – Transforming growth factor beta

TR – thyroid hormone receptor

VPA – Valproic acid

Keywords: Mixture testing; Adverse outcome pathway; Developmental toxicity;

## 1. Introduction

### *1.1 Cumulative risk assessment*

On a daily basis, people are exposed to complex mixtures of man-made chemicals, such as pesticide residues which are present in the diet. Many of these chemicals may cause health effects when dosed at a sufficiently high level. However, based on initial risk assessment, exposure can generally be expected to be well below adverse health effect limits with a low associated health risk. Nevertheless, mixtures of chemical substances may cause a combined effect even at a presumed safe level of the individual compounds. This problem of cumulative risk assessment is well recognized in toxicology, and several initiatives have been developed worldwide to address the issue. Some regulations and directives already require mixture assessment, although there is no internationally accepted harmonized strategy for cumulative risk assessment across these initiatives and regulations [1]. In recent years, one of the strategies for cumulative risk assessment was adopted by the European Food and Safety Authority (EFSA).

The EFSA strategy is based on grouping chemicals according to toxicological characteristics, the so-called cumulative assessment groups (CAG) [2] [3] [4]. The idea is that chemicals that can induce similar phenotypical effects should be grouped, while chemicals that only act on different systems in the organism are excluded. A first tier in this grouping comprises the target organ or target biological system in the organism (CAG level 1). CAG level 2 then considers the specific toxicological phenotype within that common target organ or system. A further refinement at level 3-4 considers integration about mode and/or mechanism of action (MOA) information. The relevance of MOA information is that simple dose addition (after correction for potency differences) can be safely assumed for chemicals with a similar MOA, whereas chemicals with dissimilar MOA in principle could act independently, or produce positive or negative interaction. This may lead to non-dose additive effects such as antagonism (a lower potency of the mixture compared to the combined single compounds) or synergism (a higher potency of the mixture compared to the single compounds). The absence of information on the toxicological MOA for many chemicals results in grouping under level 2 based on phenomenological effects [5]. A second consequence of the absence of information on toxicological MOA for many chemicals is that EFSA proposed dose addition as a default assumption for cumulative risk assessment [4]. This is considered a conservative approach because dose addition or less-than-dose-addition was more commonly observed compared to more-than-dose-addition in case-studies with mixtures in models relevant to human risk assessment [6, 7].

The EU-funded Horizon2020 project “EuroMix” (European Test and Risk Assessment Strategies for Mixtures; https://www.euromixproject.eu/) has elaborated on the EFSA strategy for cumulative risk assessment in proof-of-principle studies, by testing of binary mixtures of chemicals belonging to selected CAGs, and with relevance to exposure of the European population via food. One such study employed the zebrafish embryo as a model for CAG level 2 effects (cleft palate/craniofacial malformations) in CAG level 1 (developmental toxicity) and confirmed dose addition as a common principle [8]. This study used a set of reference compounds with known *in vivo* developmental effects on the formation of the head skeleton [5].

The transparent appearance of the zebrafish (*Danio rerio*) embryo enables the microscopic study of skeletal formation. In addition, the zebrafish embryo is a non-licensed experimental organism under current legislation. This renders the zebrafish embryo an excellent model for the study of skeletal development and (toxicant-induced) craniofacial malformations. Despite the differences in skeletal developmental processes (e.g. specific ossification) and the final anatomy of the craniofacial area between and within taxonomic classes, molecular pathways in embryonic development, including the pharyngeal area, are highly conserved among vertebrates.

In the previous study [8], well-defined MOA information was only available for a subset of the tested reference compounds in the present study (Table 1, Table 2), which rendered classification of mixtures as similar or dissimilar MOA approximate in some cases. Therefore, the aim of the present study was to improve this classification with the use of simple experimental models since this could help predict a (newly produced) compound’s contribution to effects in combined exposures.

*1.2 MOA to advance classification of chemicals in mixtures*

Full MOA assignment requires comprehensive analysis of genome-wide differential gene expression, preferably of multiple groups of chemically-related substances, in a dose-dependent manner and ideally in a number of models (both simple and complex) relevant to the toxicological phenotype under study. Since this was not achievable within the limitations of the project, we applied an alternative approach, including identification of major MOAs involved in craniofacial malformations and known reference compounds for these, arrangement of these MOAs in an integrated pathway network, and identification of potentially informative marker genes herein. Next, expression of these marker genes was tested for distinctive potential in zebrafish embryos exposed to reference compounds for the identified major MOAs. Expression of the most informative marker genes was then analyzed in zebrafish embryos exposed to test compounds with unknown MOAs, to achieve mapping of these compounds to known MOAs. To support our findings, the results of this marker gene expression were compared to existing activation profiles of reference and test compounds in ToxCast *in vitro* assays. In addition, the gene expression results were substantiated with *in silico* analysis of binding affinities (molecular docking modeling) of all compounds to selected biomolecules associated with initiation of the major MOAs.

*1.3 Identification of MOAs related to craniofacial malformations and synthesis of pathways into a network*

A literature search to identify MOAs related to craniofacial malformations, including cleft palate, mainly retrieved developmental toxicity studies in classical rodent-based models (Table 1).

Both the disturbance of the retinoic acid (RA) balance and activation of the aryl hydrocarbon receptor (AhR; predominantly AhR-2) are long-established causes of developmental craniofacial malformations [9, 10], and could therefore be included as major interactions in the pathway network (Fig. 1). In this line, inhibition of the RA metabolizing enzyme Cyp26 through triazoles and disruption of AhR-signalling through AhR ligands (dioxin-like acting compounds) can be understood as a cause of developmental craniofacial malformations in zebrafish [8, 11, 12] and rodents [9, 13]. Molecular pathways for both MOAs are well described, including the role of inhibition of Cyp26A and B in causing a disbalance of RA and subsequent effects on regulation of hox(n) genes [14], and effects on EGF/TGFβ3 signaling following AhR activation [15]. AhR also regulates sox genes, and in particular involvement of sox9a in cartilage morphogenesis [16] and of sox9b in AhR-related jaw malformations in zebrafish embryos [17] has been established. Additionally detected MOAs include inhibition of histone deacetylases (HDAC) [18] (with a specific role in skull morphogenesis for HDAC8 [19]), modification of folate antagonism [20], induction of oxidative stress [21], inhibition of lysyl oxidase [22], metal chelation [23, 24], and activation of peroxisome proliferation activated receptors (PPARs; an important MOA for perfluoroalkyl acids, such as PFOA and PFOS [25-29]).

Table 1 – Reference chemicals for craniofacial malformation and related major modes of action

| Chemical Class | Compounds | Modes of Action[1] |
|---|---|---|
| triazoles (3AZ) | Cyproconazole<br>flusilazole<br>hexaconazole<br>triadimefon | • **inhibition of Cyp26 (RA catabolism, increase of endogenous RA)** [30, 31]<br>• inhibition of sterol biosynthesis *via* Cyp51 inhibition [30, 31], decreased serum cholesterol [32, 33]<br>• oxidative stress [32, 34, 35] (only confirmed for flusilazole in [36])<br>• thyroid hormone disruption [35, 37, 38] |
| synthetic retinoids, RAR agonist | AM580 | • **selective RARα activator** [39] |
| synthetic retinoids, RXR agonist | CD3254 | • **selective RXR activator** [40] |
| dioxin-like compounds | TCDD | • **activation of AhR [10, 15, 41]**<br>• oxidative stress [42] |
| organic acids | valproic acid | • **histone deacetylase (HDAC) inhibition** [21]<br>• oxidative stress [21]<br>• folate antagonism [21]<br>• PPAR activation [43, 44]<br>• altered RA metabolism *via* rbp4 downregulation [45] |
| perfluorinated compounds | PFOS | • **PPAR activation** [29, 46] [29]<br>• thyroid hormone disruption [47, 48] |
| dithiocarbamates | maneb<br>metam<br>thiram | • **heavy metal chelation** [23, 49]<br>• **lysyl oxidase inhibition** [50]<br>• TGF-β1 signaling [51] (regulated by loxl [52])<br>• thyroid hormone disruption [53] |

[1.] MOA information derived from literature. MOAs in bold represent known primary MOAs. Cyp, cytochrome P450; RA, retinoic acid; RAR, retinoic acid receptor; RXR, retinoid-X receptor; TCDD, 2,3,7,8-Tetrachlorodibenzo-p-dioxin; AhR, aryl hydrocarbon receptor; PFOS, perfluorooctanesulfonate; PPAR, peroxisome proliferator-activated receptor; rbp, retinol binding protein; further gene codes are explained in Table 3.

Valproic acid (VPA), a known HDAC inhibitor, may also interact with coenzyme-A, forming a conjugate which inhibits Cpt1, and thus contributes to VPA-induced malformations [54]. Disruption of cholesterol synthesis may also be a contributory factor, as cholesterol plays a functional role in craniofacial development [55]. 14α-Sterol demethylase (Cyp51) is in vertebrates involved in cholesterol synthesis, and CYP51 knock-out mice also show craniofacial malformations [56]. Cyp51 is the intended (pharmacological) target of triazole fungicides, to inhibit ergosterol synthesis in fungi [57], and its isoform in zebrafish also has an affinity for triazoles [58].

Some reference compounds have a primary MOA related to developmental craniofacial malformations, such as potent AhR activation in the case of TCDD and other dioxin-like compounds. However, other compounds may have additional MOAs to the major mechanism underlying developmental craniofacial malformation (Table 1), such as the dithiocarbamates, which, apart from lysyl oxidase inhibition may affect skeleton formation through heavy metal (copper) chelation, and yet other pathways [22]. Similarly, other teratogens under study may also exhibit multiple MOAs including disruption of the hypothalamus-pituitary-thyroid (HPT) axis with triadimefon in addition to Cyp26 inhibition, or PPARα activation in addition to histone deacetylase inhibition with VPA. In this respect, it is not always clear whether effects on craniofacial formation can be attributed to a primary MOA.

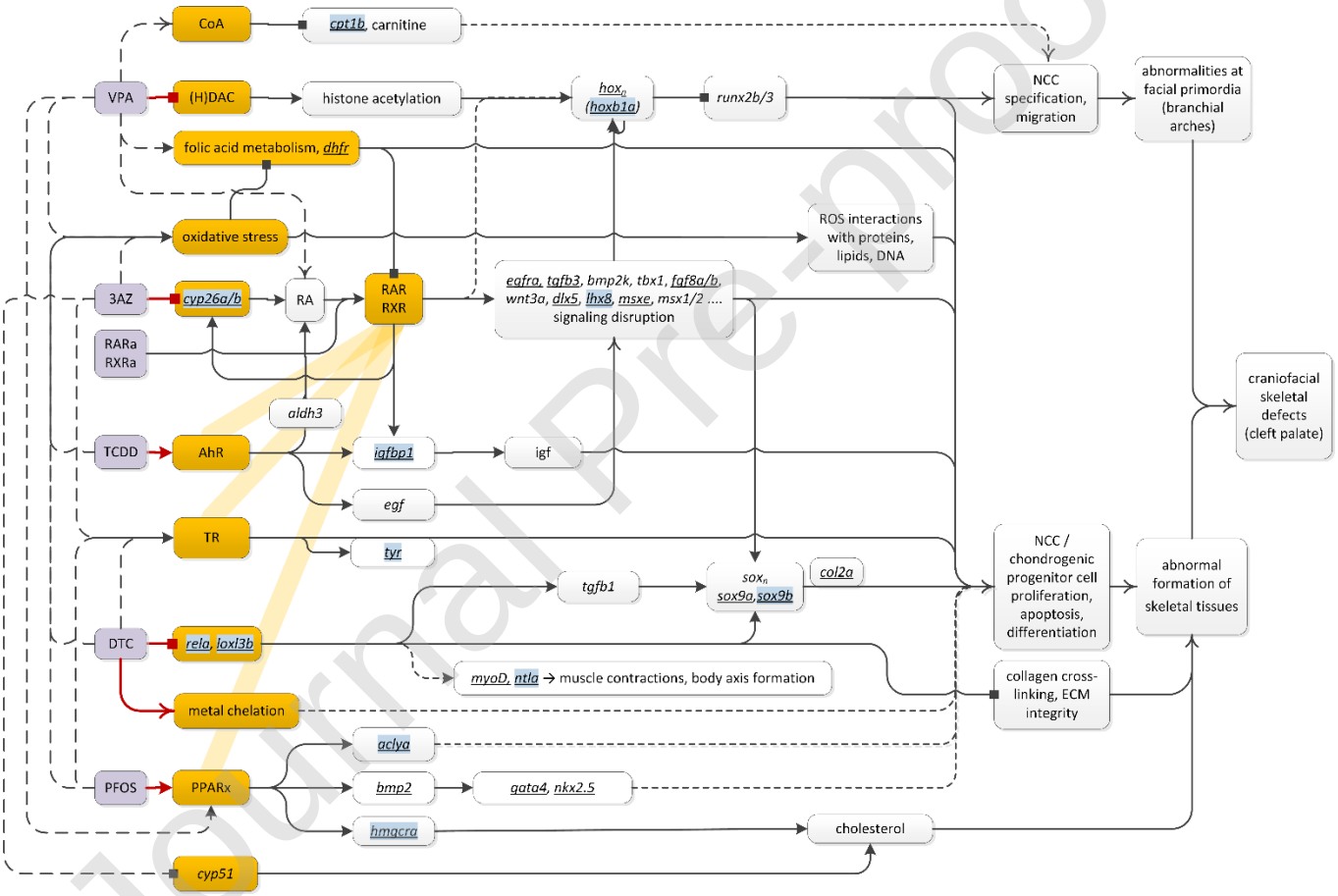


Fig. 1 – Test compounds and marker genes in MOA pathways involved in craniofacial malformations in zebrafish. Initial targets are in orange blocks, reference modulators in purple blocks. Major interactions of modulators are given with red solid connectors; minor/additional interactions are with dashed connectors. Downstream interactions are given with solid connectors when well-established, or with dotted connectors when less evident. The interaction of nuclear receptors is represented by thick orange lines. Solid arrows, stimulation/activation/increase; block connectors, inhibition/decrease; open arrows, alteration/modulation/disruption. Abbreviations of all genes and most ligands and targets are explained in Tables 2 and 3; RARa and RXRa refer to specific agonists for the RAR- and RXR-alpha variant. Potential marker genes are in italic, the tested subset is underlined, and the selection used for final distinction marked blue.

All reference compounds appear to induce further activities, such as effects on fatty acid, steroid, and xenobiotic metabolism pathways [59, 60] or inhibition of voltage-gated calcium channels by triazoles [36] or VPA [61]. Although such MOAs may indirectly contribute to craniofacial malformations, these are assumed to be of minor relevance compared to the above MOAs and are therefore not considered further.

*1.4 Marker genes in MOAs*

Upon identification of major MOAs, key genes from the molecular pathways underlying these MOAs were derived from literature. These served as potential marker genes for further qPCR analysis in the zebrafish embryos. Specifically, this included triazole-related regulation of the RA pathway [30, 66, 67, 71, 86, 87], dioxin toxicity [15, 17, 88] and downstream signalling pathways [89], the lysyl oxidase pathway and the related dithiocarbamate-induced disturbance of body axis formation [22, 23, 51, 90], PFAA-induced developmental toxicity [83, 84, 91-94], thyroid hormone disruption [95], the valproic acid adverse outcome pathway [21, 54, 96-100], and relevant genes related to oxidative stress [20, 97]. Further potential marker genes were derived from literature reviewing molecular epidemiological studies, identifying genes associated with oral clefts in man [82]. Mouse and zebrafish homologs were retrieved for these genes, for comparison with other databases and application in this study. This list was then analyzed for overlap with modes of actions or pathways, which are involved in craniofacial fusion [15], RA signaling [101], and craniofacial development in zebrafish [102]. Based on the overlap and/or specificity among these databases, a subset of 68 genes was selected as a deliverable for the EuroMix project (Table S1) [62]. A final sub selection from this list for actual testing was further fed by re-analysis of our database of previously performed genome-wide expression analysis in zebrafish embryos, with a wide array of reference compounds [66, 86, 100]. The most promising marker genes from the optimized list, which were retained after repeated testing for actual evaluation, were aligned along the assembly of all considered pathways leading to craniofacial malformations in Fig. 1. This arrangement shows that most marker genes have a functional role in the pathway network, although other genes, such as tyr or myod, have no specific or a restricted function in zebrafish head skeleton formation, and just serve as sentinels for pathway activation.

The resulting array of marker genes (Table 3) set the stage for testing and optimization in whole-body mRNA extractions in zebrafish embryos exposed for 72 hours to a set of reference compounds with well-known major MOAs, as well as a set of test compounds with unknown MOAs, all known to induce craniofacial malformations. This gene expression was compared to existing ToxCast *in vitro* activity, and to *in silico* molecular binding analysis, to accommodate the aim of the study to distinguish similar and dissimilar MOAs in view to support modeling of dose-addition in combined exposure toxicity.

## 2. Materials and Methods

### *2.1 Compound selection*

A set of reference compounds was compiled based on data available in the literature linking the compounds to the induction of craniofacial malformations (see Table 1).

### *2.2 Zebrafish*

Zebrafish (*Danio* rerio) were held and bred at the RIVM laboratory under permit NVWA-32600, according to Dutch regulations. Experiments were done with two populations of wild-type (WT) zebrafish. One population was obtained through commercial import from Singapore (referred to as RIVM-WT strain below). The second population of zebrafish was obtained from the Karlsruhe Institute of Technology (KIT, Karlsruhe, Germany; AB-strain). These populations were maintained and propagated in our facility for more than 10 or 2 generations, respectively. Fish were kept in 7.5 L ZebTec tanks (Tecniplast S.p.A., Bugugiate, Italy) at a temperature of 28 ± 1 $^{o}$C, a pH of 7.5 ± 0.5 and a conductivity of 500 ± 100 µS. In the zebrafish facility, a 14/10h light/dark photoperiod is maintained, with light intensity being gradually dimmed/increased over a 30-min period. The fish were fed twice daily with SDS 100, 200, or 400 (Tecnilab BMI, Someren, the Netherlands) depending on the age of the fish. Zebrafish larvae and young adults received supplementary live *Artemia salina* (artemia; in-house culture), and adult fish daily received defrosted artemia (Tecnilab BMI, Someren, the Netherlands).

One day prior to spawning, male and female zebrafish were transferred to 3.5L breeding tanks at a ratio of 3:3 per tank. Shortly after spawning fertilized eggs were collected in a petri dish and rinsed thoroughly with Dutch standard water [12]. The quality of the eggs was checked microscopically and batches with less than 10% coagulated eggs and limited egg deformations were pooled and used for experiments, after removal of coagulated eggs. Around three hours post-spawning, pools of 15 embryos per well were exposed in 6-wells plates in 5 mL medium consisting of solvent control or a single concentration of a test compound (Table 2), with 6-10 replicate wells for each control and compound. All compounds were dissolved in 0.1% v/v DMSO. Pilot experiments learned that testing gene regulation at 72 hours post-fertilization (hpf) provides sufficient resolution. Therefore, these pools of embryos were euthanized at that time, and snap-frozen in liquid nitrogen and stored at -80°C.

### *2.3 Determining concentrations for gene expression analysis*

For comparison of differential gene expression among compounds, single, equipotent, concentrations were used for the gene expression experiments (Table 2). Equipotent concentrations were defined as the dose inducing a 20% effect size for induction of critical effects on the head skeleton (CED20) measured by a change in the angle formed by the Meckel's and palatoquadrate cartilages (M-PQ angle). These effects were assessed using the alcian blue staining at 120hpf to visualize the cartilaginous skeleton [8, 12]. Previously reported dose-response data of these M-PQ measurements [8, 12] were re-analyzed to obtain CED20s, see Fig. 2 for illustration. The CED20 was analyzed separately in RIVM-WT and AB fish, to account for sensitivity differences among these strains.

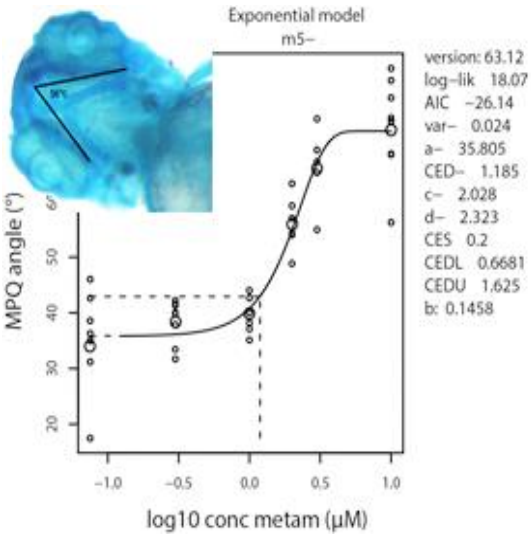


Fig. 2 – Definition of the concentration for gene expression, illustrated in the case of metam. Measurement of the MPQ angle (defined as the angle formed by the rostral tip of Meckel's cartilage and the joint of the palatoquadrate-ceratohyal cartilages [12]) is shown in the insert (zebrafish embryo head, exposed with 3 µM metam, at 72hpf). Each small circle in the dose-response graph represents a measurement in a single embryo, large circles are group means. The horizontal dotted line is the 20% effect level (CES 0.2), relative to background (a = 35.8°). The intersection with the curve fit determines the critical effect dose (CED), in this case 1.2 µM, which is then used as the concentration for gene expression analysis.

*2.4 Gene expression analysis*

For RNA isolation, the RNeasy microarray tissue kit (QIAGEN, Hilden, Germany) was used according to the manufacturer's protocol. Briefly, frozen embryos were homogenized and lysed in Qiazol, chloroform was added, mixed and centrifuged. The aqueous phase was mixed with EtOH (70%), RNA was extracted and DNase treatment was included. The integrity and purity of the isolated RNA was checked using the Bioanalyzer 2100 (Agilent, Waldbronn, Germany) and NanoDrop 1000 (Thermo Fisher Scientific, Waltham MA, USA) instruments. Samples with an RNA Integrity Number (RIN) between 7 and 10 were considered of sufficient quality for further qPCR experiments.

*2.5 Analysis of gene expression by RT-qPCR*

The High-Capacity cDNA Reverse Transcription Kit (Thermo Fisher Scientific) was used according to the manufacturer's protocol to synthesize cDNA from RNA isolates. Subsequently, quantitative real-time PCR was performed using a 7500 FAST Real-Time PCR System with Taqman gene expression assays and Taqman FAST universal PCR master mix used according to the manufacturer's protocol (all Thermo Fisher Scientific). The RT-PCR program used consisted of 10 minutes at 25 °C, followed by 2 hours at 37 °C, then 5 minutes at 85 °C after which the temperature was kept at 4 °C. The product of this RT-PCR reaction was diluted at a ratio of 1:1 with water. For the subsequent qPCR, 5 µL PCR product was mixed with 15 µL TaqMan™ assay premix consisting of 4 µL nuclease-free water, 10 µL TaqMan™ fast Universal Primer and 1 µL target-specific TaqMan™ 20X assay mix. Glyceraldehyde 3-phosphate dehydrogenase (*gapdh*), hypoxanthine phosphoribosyltransferase 1 (*hprt1)* and actin beta 1 (*actb1)* were used as

reference genes. Relative expression levels were calculated using the $2^{-\Delta\Delta CT}$ method [62], which considers the expression of each marker genes compared to the mean expression of the three reference genes and the compound-induced expression compared to background expression level in blank controls. The resulting fold change values were expressed as log2FC, then normalized to the strongest regulated gene per compound. All transformations are shown in Table S3. The list of genes analyzed by RT-qPCR is given in Table 3.

Table 2 – Technical details and equipotent test concentrations of reference- and test compounds

| Compound | Full names | CAS# | Purity | Equipotent test concentrations (μM)[4] |
|---|---|---|---|---|
| ***Reference compounds*** | | | | |
| AM580 | 4 - [[(5,6,7,8 - Tetrahydro - 5,5,8,8 - tetramethyl2-naphthalenyl) carbonyl]amino]benzoic acid | 102121-60-8 | >98% | 0.0028 |
| Boric acid | Hydrogen borate | 10043-35-3 | >99.5% | 6.3 |
| CD3254 | 3-[4-Hydroxy-3-(5,6,7,8-tetrahydro-3,5,5,8,8-pentamethyl-2-naphthalenyl)phenyl]-2-propenoic acid | 196961-43-0 | >97% | 0.077 |
| Cyproconazole | 2-(4-Chlorophenyl)-3-cyclopropyl-1-(1H-1,2,4-triazol-1-yl)-2-butanol | 94361-06-5 | 97.2% | 40 / 170 |
| Flusilazole | 1-((bis(4-fluorophenyl)methylsilyl)methyl)-1H-1,2,4-triazole | 85509-19-9 | Analytical standard | 6.5 / 17.2 |
| Hexaconazole | 2-(2,4-Dichlorophenyl)-1-(1H-1,2,4-triazol-1-yl)hexan-2-ol | 79983-71-4 | >99.3% | 21.1 |
| Maneb | Mangaanethyleenbis dithiocarbamate | 12427-38-2 | 90.8% [3] | 0.6 |
| Metam | natrium-N-methyl dithiocarbamate | 137-42-8 | 70.8% [3] | 1.2 |
| PCB126 | 3,3',4,4',5-Pentachlorobiphenyl | 57465-28-8 | Analytical standard[1] | 0.044 |
| PFOS | 1,1,2,2,3,3,4,4,5,5,6,6,7,7,8,8,8-Heptadecafluoro-1-octanesulfonic acid | 1763-23-1 | Analytical standard | 10 / 92 |
| TCDD | 2,3,7,8-Tetrachlorodibenzo-p-dioxin | 1746-01-6 | 100% | 0.0013 / 0.01, 0.1 |
| Thiram | dimethylcarbamothioylsulfanyl- N,N-dimethyl dithiocarbamaat | 137-26-8 | Analytical standard | 0.014 / 0.1 |
| Triadimefon | 1-(4-Chlorophenoxy)-3,3-dimethyl-1-(1H-1,2,4-triazol-1-yl)butan-2-one | 43121-43-3 | Analytical standard | 6.6 / 62.0 |
| Valproic acid | 2-Propylpentanoic acid | 99-66-1 | 100% | 120 / 1633 |
| ***Test compounds*** | | | | |
| 2,4-dinitrophenol | 2,4-dinitrophenol | 51-28-5 | 99.9% | 19.9 |
| Endosulfan | 1,2,3,4,7,7-hexachloor-8,9,10-trinorborn-2-een-5,6-yleendimethylsulfiet | 115-29-7 | Analytical standard | 0.32 / 0.21 |
| Fenpropimorph | cis-4-[(RS)-3-(p-tert-butylfenyl)-2-methylpropyl]-2,6-dimethylmorfoline | 67564-91-4 | Analytical standard[2] | 15.7 / 25.9 |
| Prochloraz | N -propyl- N -[2-(2,4,6-trichlorophenoxy)ethyl]-1 H - imidazole-1-carboxamide | 67747-09-5 | 98.6% | 10.1 / 15.5 |
| RA | (2E,4E,6E,8E)-3,7-dimethyl-9-(2,6,6-trimethylcyclohexen-1-yl)nona-2,4,6,8-tetraenoic acid | 302-79-4 | >98% | 0.16 |

[1] gift from Dr. Patrik Andersson, Umeå University, Sweden; originally purchased from Neosyn Inc. (New Milford CT, USA), and purified at Dr. Andersson's lab. [2] purchased from LGC Standards. [3] The low purities of metam and maneb are due to water impurity. [4] Test concentrations for mRNA analysis were CED20s for head skeleton malformation and show sensitivity differences between RIVM-WT and AB fish which are separated by /. In AB fish, TCDD was tested at two concentrations to account for variation in repeated CED20 analysis.

Table 3 - Tested marker genes

| Target | Gene name | Assay ID | Function of gene | Targeted MoA | Reference |
|---|---|---|---|---|---|
| *Retained marker genes* | | | | | |
| ***cyp26a1*** | Cytochrome P450 26A1 | Dr03086662_m1 | RA binding | RA metabolism | [63] |
| ***cyp26b1*** | Cytochrome P450 26B1 | Dr03088547_m1 | RA binding | RA metabolism | [63] |
| ***dlx5a*** | Distal-less homeobox 5a | Dr03150313_m1 | transcription factor | RAR/RXR activation | [64-67] |
| ***hoxb1a*** | Homeobox B1a | Dr03124995_m1 | transcription factor | RAR/RXR activation | |
| ***igfbp1b*** | Insulin-like growth factor binding protein 1b | Dr03073589_m1 | Insulin-like growth factor binding | RA metabolism / homeostasis | [63] |
| ***lhx8a*** | LIM homeobox 8a | Dr03076496_m1 | transcription | RAR/RXR activation | [68] |
| ***loxl3b*** | Lysyl oxidase-like3b | Dr03429934_m1 | copper ion binding; fibronectin binding; protein-lysine 6-oxidase activity; scavenger receptor activity | Lysyl oxidase inhibition; extracellular matrix formation | [24] |
| ***sox9a*** | SRY (sex determining region Y)-box 9a | Dr03112282_m1 | transcription factor | AhR activation | [66] |
| ***sox9b*** | SRY (sex determining region Y)-box 9b | Dr03080049_m1 | transcription factor | AhR activation | [66] |
| ***ntla*** | no tail-a (T-box transcription factor T-A) | Dr03086668_m1 | transcription factor | Lysyl oxidase inhibition | [66, 69] |
| ***tyr*** | Tyrosinase | Dr03138104_m1 | hydroxylation of tyrosine | target of thyroid hormone / at RA signaling | [70, 71] |
| ***rela*** | Nfkb3 | Dr03114752_m1 | transcription factor | loxl, ntla regulation | |
| ***dhfr*** | Dihydrofolate reductase | Dr03131624_m1 | DNA synthesis | Folate metabolism | [72] |
| ***aclya*** | ATP citrate lyase a | Dr03121245_m1 | fatty acid / acetyl CoA synthesis | PPARγ activation / fatty acid synthesis | [73, 74] |
| ***hmgcra*** | 3-hydroxy-3-methylglutaryl-CoA reductase a | Dr03428701_m1 | cholesterol synthesis (acetyl-CoA consumption) | Sterol metabolism | [75, 76] |
| ***cpt1b*** | carnitine palmitoyltransferase 1B | Dr03147243_m1 | fatty acid beta-oxidation | Fatty acid metabolism | |
| *Marker genes rejected after testing* | | | | | |
| ***egfra*** | epidermal growth factor receptor a | Dr03144700_m1 | binding of extracellular ligands | AhR activation, RA pathway | [67] |
| ***fgf8a*** | fibroblast growth factor 8a | Dr03105657_m1 | signal peptide | RAR/RXR activation | [64, 66, 77] |
| ***fgf8b*** | fibroblast growth factor 8b | Dr03433601_m1 | signal peptide | RAR/RXR activation | [65, 66, 77] |
| ***hoxa2b*** | homeobox A2b | Dr03112035_m1 | transcription factor | RAR/RXR activation | [66, 78] |
| ***tgfb3*** | transforming growth factor, beta 3 | Dr03093762_m1 | signal peptide | RAR/RXR, AhR activation | [66, 67] |
| ***msxe*** | muscle segment homeobox 1a | Dr03986683_uH | transcription factor | RAR/RXR activation | [64-67] |
| ***col2a1*** | collagen type 2 alpha 1 | Dr03099235_m1 | cartilaginous collagen | Lysyl oxidase inhibition | [23, 79] |
| ***myod*** | Myogenic differentiation | Dr03138242_g1 | transcription factor | Lysyl oxidase inhibition | [23, 79] |
| ***bmp2k*** | bone morphogenetic protein 2 | Dr03102638_m1 | signal peptide | PPAR, AhR activation | [15, 79, 80] |
| ***nkx2.5*** | nk2 homeobox 5 | Dr03074126_m1 | transcription factor | PPAR activation | [66, 80, 81] |
| ***gata4*** | GATA binding protein 4 | Dr03443262_g1 | transcription factor | PPAR activation | [80] |
| *housekeeping genes (for reference)* | | | | | |
| ***actb1*** | actin beta 1 | Dr03432610_m1 | | | |
| ***gapdh*** | glyceraldehyde-3-phosphate dehydrogenase | Dr03436842_m1 | | | |
| ***hprt1*** | hypoxanthine phosphoribosyltransferase 1 | Dr03095135_m1 | | | |

For further abbreviations, see legend to Table 1. References refer to the link between a gene and skeletal malformations.

*2.6 Analysis of qPCR data, optimization of the marker array*

The identification of an informative set of expression markers was achieved through several rounds of differential gene expression analysis. Each round included a selection of reference compounds tested in 13-15 test genes. The first round was a selection of assumed key genes from the list resulting from the literature search [82]. Marker genes were then assessed in an iterative process of retaining the most informative genes, removing non-informative genes including non-responsive genes, non-discriminative genes (*i.e.* genes responding with all compounds), genes with highly variable responses within a compound class. Each round, new candidate marker genes were added.

For most compounds, the analysis with the final array of marker genes was repeated at least once, and the number of replicates was higher when considering compound classes, mounting up to eight in the case of triazoles. Since the purpose of the analysis was to compare gene expression profiles among classes of compounds, available replicate values of differential expression were averaged per reference compound class. Subsequently, data were normalized to the strongest response across the tested marker genes, per compound class and finally expressed as percentages. All data were included in these transformations, including deviating experiments, irrespective of the statistical significance of the original per experiment differentially expressed genes, to achieve an unbiased representation of the net effect in the final result, serving as a template to match gene expression profiles of test compounds.

*2.7 Compound activity in ToxCast*

Further support for compound MOA was sought through activity analysis in the ToxCast database (https://comptox.epa.gov/dashboard/chemical_lists/toxcast Accessed Oct 15, 2019) [83]. Activity records for all compounds of interest, as far as available in the database, were downloaded and screened for testing in assays relevant to this study. Included activity parameters were RAR*, RXR*, PPAR*, TR*, AhR*, and HDAC.

*2.8 Molecular docking, binding energies, and affinities.*

To assess potential docking and binding of compounds to receptors and enzymes in the MOA pathways (Fig 1), the primary structures of the selected zebrafish receptor proteins were downloaded from the UniProt Protein Knowledgebase database. After a BLAST search of the Protein Data Bank database for homologs to the selected proteins, the crystallographic structures reported in Supplementary Table S2 were set as templates. All the alignments produced by the Clustal Omega software were manually checked. All the comparative models were produced with the MOE Homology Model program of the Protein module with default settings, also importing the ligands co-crystallized with the template proteins. The quality of the final models was carefully checked with the MOE (Molecular Operating Environment) Protein Geometry program. The two zebrafish HDAC6 (PDB ID: 5EEI) and HDAC10 (PDB ID: 5TD7) crystallographic data were downloaded from the Protein Data Bank and structure-prepared using MOE Structure Preparation program, in order to solve any crystallographic errors and to add any missing atoms.

The binding sites of the selected proteins were identified through the MOE Site Finder program, which uses a geometric approach to list putative binding sites in a protein, starting from its three-dimensional structure while checking the correspondence with the co-modeled ligand.

Selected chemicals were downloaded from the PubChem database. Each molecule was converted into a three-dimensional structure, and energy minimized, with the MOE Energy Minimize program, down to an RMS gradient of 0.05 kcal/mol/Å2. The stereochemistry of each structure was carefully checked. Molecular docking was carried out through the MOE Dock program. The Triangle Matcher placement algorithm was selected, and the London dG empirical scoring function was used for sorting the poses. The 30 top-scoring poses were refined through molecular mechanics, considering each receptor as a rigid body, and the refined complexes were scored through the GBVI/WSA dG empirical scoring function, selecting the five top-scoring poses and estimating their binding free energy (ΔG) to the ligand-binding domain of the selected proteins. A further refinement was carried out for all the receptors and enzymes connected with the identified MOAs craniofacial malformations, estimating the binding affinity of the complexes with the MOE QuickPrep program, which allows to re-score the docking poses.

The estimated binding affinity of the top-scoring solution for all the receptors and enzymes connected with the identified MOAs of craniofacial malformations was not directly computed from the GBVI/WSA dG value, but the complexes were further refined through the use of a set of specific procedures aimed at the minimization of ligands in the protein binding site. Finally, the dissociation constant ($K_i$) was computed starting from empirical binding free energy values according to the following equation:

$$\Delta G = RT \ln(K_i)$$

where R represents the gas constant and T the temperature in Kelvin, $K_i$ was computed starting from the affinity values at a fixed temperature (300K)

*2.9 Statistical analysis.*

To derive equipotent 20% effect concentrations (CED20; Table 2) from the MPQ dose-response data, exponential models were used (PROAST package (v63.12 or higher) in R (v3.5.1)) [84]. PROAST applies a goodness-of-fit to test for statistical significance of the output. Statistical significance in the gene expression data was tested using a T-test ($p$<0.05) comparing the untransformed expression values per gene in compound-exposed and control samples.

Regulation of gene expression was tested for statistical significance using a T-test (P<0.05; R statistical software) to compare untransformed expression values per gene in compound-exposed and control samples. Informative quality of the genes to distinguish groups of reference compounds was assessed in initial rounds through informed assessment of gene expression, assisted by hierarchical cluster analysis of statistically significantly regulated marker genes (P<0.05, T-test) using Euclidean distance and Ward.D linkage (R statistical software). In the final array, this informative quality was tested for statistical significance using a T-test (P<0.05) to compare the expression per gene in each compound class with the expression across the remainder of compounds.

## 3. Results

### *3.1 Gene expression profiles of reference compounds*

All reference and test compounds were analyzed for effects on the expression of the final selection of marker genes, as derived from the MOA network associated with craniofacial malformations (see 1.3, Table 3). Some genes showed a consistent pattern of regulation across replicates within a compound class, e.g. c*yp26a1* upregulation in triazoles, or *sox9b* downregulation in TCDD (Table 4A; Supplementary Table 3). Consistent or nearly consistent responses can be considered robust and are marked bold in summary Table 4B. Other genes showed a more variable result, mostly observed for weaker connections in the MOA network, such as *tyr* or *ntla* (Fig. 1). The examples of the triazole and dioxin classes (Table 4A) show that some genes have notable variation (*e.g. igfbp* in the triazoles), or occasional deviation (*e.g. rela* in hexaconazole), or that an entire single experiment deviates (e.g. the first PCB 126 experiment, Table S3).

In this way, expression of most marker genes confirmed their anticipated function in dedicated pathways. Deviations, however, were observed, such as the absence of a response in *rela* and *loxl3b* with dithiocarbamates, which can be understood from biological and technical reasons, such as unmatched sensitive window (see Discussion). This may also apply for the 11 marker genes that did not show the predicted response, and also had no further discriminative potential. These markers were therefore excluded from the final marker list (Table 3). Further, *igfbp1b* and *dlx5a* were consistently counter-regulated (notably in the RAR, RXR, and RA profiles), and therefore the one with the weakest response (*dlx5a*) does not add to the discriminative power of the whole set.

There were no remarkable differences observed between the two used strains of zebrafish, i.e. the AB strain (Table 4A; marked CS in Table S3) and the RIVM-WT strain (other experiment marks in Table S3). This is in line with the adjustment of used test concentrations per strain to account for sensitivity differences (Table 1), rendering it possible to combine the gene expression profiles from these strains.

Table 4A – Reproducibility of differential gene expression within the triazole and dioxin classes of reference compounds

| | | *cyp26a1* | *cyp26b1* | *dlx5a* | *hoxb1a* | *igfbp* | *lhx8a* | *loxl3b* | *sox9a* | *sox9b* | *ntla* | *aclya* | *cpt1b* | *dhfr* | *hmgcra* | *rela* | *tyr* | **ZF strain** |
|---|---|---|---|---|---|---|---|---|---|---|---|---|---|---|---|---|---|---|
| Triazoles | Cyproconazole | 100 | 78.3 | -4.3 | 36.8 | -40.4 | 8.3 | 13.3 | 5.8 | 38.1 | 4.6 | -1.5 | -12.0 | 3.5 | -28.3 | 25.3 | 13.8 | RIVM |
| | Cyproconazole | 100 | 81.0 | 0.7 | 40.5 | 46.6 | -9.1 | -11.0 | -4.1 | -5.0 | 5.4 | 0.0 | 0.0 | 0.0 | 0.0 | 0.0 | 0.0 | RIVM |
| | Cyproconazole | 100 | 56.3 | -30.9 | 53.5 | 90.3 | -37.3 | -48.1 | -30.1 | -13.1 | 8.3 | -7.7 | -47.7 | -40.6 | 6.7 | 16.7 | 7.0 | AB |
| | Flusilazole | 89.6 | 100 | -6.6 | 23.1 | 30.1 | -12.0 | -14.8 | -5.8 | -4.3 | 10.4 | 2.5 | -1.5 | 6.6 | 4.6 | -11.2 | 4.2 | RIVM |
| | Flusilazole | 100 | 67.3 | -18.3 | 26.4 | 32.0 | -31.7 | -30.6 | -30.4 | -18.8 | 14.3 | -12.4 | -3.9 | -16.3 | -2.5 | -2.6 | -0.3 | AB |
| | Hexaconazole | 78.9 | 30.1 | -17.0 | -3.6 | -21.5 | -14.7 | -20.4 | -11.3 | -2.6 | 6.0 | -13.5 | -29.9 | 18.5 | 8.0 | -100 | 9.9 | RIVM |
| | Triadimefon | 68.4 | 100 | 7.0 | 48.5 | -14.4 | -7.9 | -10.4 | 2.6 | 18.8 | 9.4 | | | | | | | RIVM |
| | Triadimefon | 100 | 73.1 | -11.3 | 32.9 | 7.7 | -17.9 | -20.5 | -23.8 | -11.9 | -2.6 | 3.7 | 8.8 | 9.5 | 34.7 | 1.2 | -5.2 | AB |
| Dioxin | TCDD | -50.7 | -33.0 | -11.5 | -63.1 | 44.6 | 65.6 | 38.7 | -10.0 | -100 | -10.5 | | | | | | | RIVM |
| | TCDD 10nM | -53.2 | -13.3 | 8.6 | 10.7 | -11.4 | 75.5 | -38.5 | -12.2 | -100 | 19.4 | 4.6 | -13.0 | -29.0 | -17.6 | 54.2 | -19.2 | AB |
| | TCDD 100nM | -65.9 | -7.5 | 6.2 | 25.3 | 51.9 | 72.8 | -75.6 | -6.3 | -100 | 47.0 | 16.0 | -30.5 | -64.4 | -40.9 | 93.1 | -12.5 | AB |

Color shading represents the intensity of regulation with blue being up and red down. Differential gene expression is expressed as log2FC, then normalized to the strongest regulated gene per compound. All transformations are shown in Table S3. Statistical significance was observed in the majority of differentially expressed genes with a log2FC exceeding ±0.1 in the original experiments (Table S3), corresponding to an approximate value of 15 after the final transformation.

Table 4B - Matching test compounds with reference profiles; see Table 4C for matching algorithm

| | | *cyp26a1* | *cyp26b1* | *hoxb1a* | *sox9b* | *igfbp* | *lhx8a* | *loxl3b* | *rela* | *ntla* | *aclya* | *cpt1b* | *hmgcra* | *tyr* |
|---|---|---|---|---|---|---|---|---|---|---|---|---|---|---|
| **Reference** | triazoles (3,2,2,1) | **100.0*** | **77.1*** | 37.2 | -5.4 | 28.7 | -20.2 | -23.1 | -1.5 | 7.1 | -4.9 | -13.0 | 8.9 | 2.6 |
| | RAR (1) | **65.5** | **-45.8** | **100.0** | **-1.7** | **-98.4** | **-36.0** | **-36.0** | -0.3 | **-15.2** | 2.0 | **-29.8** | **16.6** | **41.2** |
| | RXR (1) | 17.2 | -18.3 | **-94.3** | -24.0 | **90.6** | 24.7 | -28.9 | 12.9 | -20.8 | **-64.1** | **-44.7** | 11.0 | -40.6 |
| | dithiocarbamates (3,2,2) | -14.7* | -6.7 | 38.4 | 51.1* | 23.0 | -0.8 | -9.3 | 1.1 | **53.1** | -23.8 | -38.4 | **-100.0*** | 10.5 |
| | AhR (3,2) | -51.1 | -25.9 | 1.3 | **-100.0*** | 15.4 | **74.8*** | -31.2 | **83.2*** | 21.6 | 6.6 | -31.4 | **-58.0** | -5.3 |
| | VPA (2) | 8.1 | -10.8 | 38.9 | 12.9 | 22.7 | **-23.7** | **30.1*** | **40.7** | **25.4** | **24.8*** | **-100.0*** | 23.1 | -7.0 |
| | PFOS (2) | 8.9 | -5.7 | 10.6 | **-65.2** | **100.0** | -6.8 | -10.3 | **-25.4** | **19.1** | -4.5 | **83.9*** | -29.4 | -5.7 |
| **Test** | 2,4-dinitrophenol (1) | -7.7 | -36.6 | -9.9 | -30.4 | -100.0 | -5.7 | 7.2 | 38.7 | 17.5 | -23.0 | -6.7 | -27.4 | -4.9 |
| | Boric acid (1) | -5.5 | -53.5 | 32.8 | -22.7 | -100.0 | -6.3 | 22.9 | 39.3 | -6.0 | -14.6 | -38.6 | 31.3 | 14.3 |
| | endosulfan (2) | **23.6** | -2.5 | 18.6 | -0.4 | **100.0** | -1.6 | -3.8 | -30.0 | **31.1** | 2.9 | **45.9** | 8.8 | **-21.9** |
| | Fenpropimorph (1) | 19.2 | -7.3 | 29.0 | 21.2 | 100.0 | -4.7 | -9.0 | -58.0 | 42.4 | 4.0 | -3.8 | -46.8 | 13.8 |
| | Prochloraz (2) | **12.8** | 5.3 | -6.4 | 5.2 | 41.5 | -5.8 | **-23.0** | 11.1 | 11.3 | -5.6 | 6.6 | **-73.9** | 16.6 |
| | RA (1) | **-2.4** | -35.9 | 10.2 | -35.0 | -14.9 | 33.1 | **-8.0** | 12.6 | 8.5 | -15.2 | -30.8 | **-100.0** | 48.6 |

Triazoles represents the average of cyproconazole (n=3), flusilazole (n=2), triadimefon (n=2), hexaconazole (n=1); RAR is AM580; RXR is CD3254; dithiocarbamates is the average of thiram (n=3), metam (n=2), maneb (n=2); AhR is average of TCDD (n=3), PCB126 (n=2); VPA, PFOS, endosulfan, and prochloraz are all average of 2 replicates. Colour shading represents the intensity and direction of regulation with blue being up and red down. Differential gene expression is in log2FC, then normalized to the strongest regulated gene per compound. All transformations are shown in Table S3. Bold figures indicate consistency of change in all replicates in reference compounds. Statistical significance was observed in the majority of differentially expressed genes with a log2FC exceeding ±0.1 in the original experiments (Table S3), corresponding to an approximate value of 15 after the final transformation. The strategy to match gene regulation of a test compound to that of reference compounds is explained in Table 4C. Values marked with an asterisk are significantly regulated (p-values ≤0.05)

Table 4C – Matching compounds to Reference MOA marker profiles

| | | profile | | | | | | |
|---|---|---|---|---|---|---|---|---|
| | | triazoles | RAR | RXR | DTC | AhR | VPA | PFOS |
| **Reference** | Triazoles | 4 | 1 | 1 | 0 | 0 | 0 | 1 |
| | RAR | 2 | 4 | 0 | 0 | 0 | 1 | 0 |
| | RXR | 0 | 0 | 4 | 0 | 1 | 1 | 1 |
| | DTC | 1 | 1 | 0 | 4 | 0 | 1 | 0 |
| | AhR | 0 | 0 | 0 | 1 | 4 | 1 | 1 |
| | VPA | 1 | 1 | 0 | 1 | 1 | 4 | 0 |
| | PFOS | 0 | 0 | 1 | 1 | 2 | 0 | 4 |
| **Test** | 2,4-Dinitrophenol | 0 | 2 | 0 | 1 | 3 | 0 | 1 |
| | Boric acid | 1 | 3 | 0 | 0 | 1 | 1 | 0 |
| | Endosulfan | 0 | 0 | 1 | 1 | 0 | 0 | 3 |
| | Fenpropimorph | 1 | 1 | 1 | 2 | 0 | 0 | 1 |
| | Prochloraz | 0 | 0 | 1 | 1 | 0 | 0 | 1 |
| | PCB126 | 0 | 1 | 0 | 1 | 3 | 1 | 1 |
| | RA | 2 | 2 | 1 | 0 | 0 | 1 | 1 |

Each of the reference MOAs was identified through one major distinctive marker (score 2) and two supporting markers (each providing a score of 1), see Table S3 for details. The respective profiles were: triazoles, *cyp26b1*↑, *cyp26a1*↑, *hoxb1a*↑; RAR, *igfbp*↓, *hoxb1a*↑, *tyr*↑; RXR, *hoxb1a*↓, *igfbp*↑, *tyr*↑; DTC, *sox9b*↑, *ntla*↑, *hmgcra*↓; AhR, *sox9b*↓, *lhx8a*↑, *rela*↑; VPA, *loxl3b*↑, *aclya*↑, *cpt1b*↓; PFOS, *cpt1b*↑, *sox9b*↓, *igfbp*↑ (major marker followed by two supporting markersfor each compound). The full profile algorithm was applied to the complete set of reference and test compounds, leading to a full match (score 4), or strong, modest, poor and no matches (respective decreasing scores 3→0).

Table 5A – Compound activity in ToxCast assays

| target | ToxCast assay name | compounds |
|---|---|---|

*3.2 Matching test compound gene expression profiles with reference profiles*

From these reference profiles, rules were derived to match profiles of test compounds, building on most prominent differentially expressed genes and considering supportive genes (Table 4C, Table S3). The most marked profiles were the triazoles, RAR-, and RXR-related genes. None of the test compounds showed the characteristic concomitant upregulation of both *cyp26a1* and c*yp26b1*, thus excluding a match with the triazoles profile. Downregulation of *igfbp* and concurrent upregulation of both *hoxb1a* and *tyr*, identifying the RAR profile, was most closely matched by boric acid, 2,4-dinitrophenol and RA. The gene expression profile related to RXR, mainly determined by evident downregulation for *hoxb1a*, wasn't matched by any of the test compounds.

The characterizing induction of *sox9b* and *ntla* observed with dithiocarbamates, combined with a marked decrease of *hmgcra* was shared by fenpropimorph. Prochloraz also had a prominent inhibition of *hmgcra,* but there was no further support for a match with the dithiocarbamate profile. Regarding regulation of the key AhR-associated markers *sox9b*, *lhx8a*, and *rela*, there was a good overlap for 2,4-dinitrophenol and PCB126. Finally, the PFOS profile resembled the endosulfan MOA, particularly through shared upregulation of *cpt1b* and *igfbp*. Thus, 2,4-dinitrophenol matched well with AhR and showed a modest match with RAR, boric acid matched strongly with RAR, endosulfan had a good match with PFOS, fenpropimorph had a modest match with the dithiocarbamate profile, prochloraz had no clear match with any profile, PCB126 matched with the AhR profile, and RA matched modestly with triazoles and RAR.

*3.3 Specific compound activities in ToxCast*

In view of the partial confirmation of anticipated markers/MOAs, and detection of unanticipated markers/MOAs, further support was sought in the ToxCast database, which holds the most complete analysis of activities of the compounds at dedicated targets in this study (https://comptox.epa.gov/dashboard/chemical_lists/toxcast, accessed March 7, 2020) [83]. All represented compounds and relevant targets are collected in Table 5A, which shows that neither of the compounds showed full coverage of testing in all ToxCast assays, up to no occurrence at all for metam. Furthermore, some targets were not included in the ToxCast database (e.g. *cyp26*), and the same is true for some compounds (CD3254, PCB 126). Nevertheless, when summarizing these data (Table 5B), a general conclusion can be drawn that complex interactions are suggested for most compounds or compound classes. This is even true for compounds with assumed selective activity, such as RXR activation by AM580 which is a specific RARα activator [39], or RAR activation by PFOS, a known PPARα activator. Further specific observations are discussed below in the context of differential gene expression.

| | | Cyproconazole | Flusilazole | Hexaconazole | Triadimefon | AM580 | TCDD | Maneb | Metam | Thiram | PFOS | VPA | 2 4-dinitrophenol | Boric Acid | Endosulfan | Fenpropimorph | Prochloraz | RA |
|---|---|---|---|---|---|---|---|---|---|---|---|---|---|---|---|---|---|---|
| RAR | ATG_RARa_TRANS_up | | 8.2 | | 41.5 | | | | | | | | | | | | 2.51 | |
| | ATG_RARg_TRANS_up | | | | | 0.08 | | | | | | | | | | | | |
| | NVS_NR_hRARa_Agonist | | | | | | | | | | | | | | | | | 0.13 |
| | NVS_NR_hRAR_Antagonist | | | | | | | 8.99 | | | 28.4 | | | | | | | |
| | NVS_NR_rAR | | | 4.3 | | | | 16.9 | | | 4.27 | | 0.54 | | | | | |
| | TOX21_RAR_LUC_Agonist | | | | | 0.023 | | | | | | | | | | | | 10.3 |
| | TOX21_RAR_LUC_Antagonist | | 67.4 | 46.3 | | | | | | 0.226 | | | | | 48.3 | | | |
| RXR | ATG_RXRb_TRANS_up | | | | | | | | | | | | | | | | | 1.0 |
| | OT_NURR1_NURR1RXRa_0480 | | | | | | | | | | | 87.1 | | | | 77.7 | 21.7 | |
| | OT_NURR1_NURR1RXRa_1440 | | | | | | | 39 | | | | | | | | 69.4 | 31.3 | 85.5 |
| | TOX21_RXR_BLA_Agonist_ch1 | | | | | | | | | | | | | | 76 | | | |
| | TOX21_RXR_BLA_Agonist_ch2 | | | | | 3.8 | | | | | | | | 17.1 | | | | 0.06 |
| | TOX21_RXR_BLA_Agonist_ratio | | | | | 0.082 | | | | | | | | 20.3 | | | | 0.026 |
| | TOX21_TR_RXR_BLA_Agonist_Followup_ratio[1] | | | | | | | | | | | | | | | | | 0.79 |
| AHR | ATG_Ahr_CIS_up | | | | 33.9 | | | | | | | | | | | 30.2 | 22.7 | |
| | TOX21_AhR_LUC_Agonist | | | | 128 | | 0.00026 | | | | | | 11.3 | | | | 0.37 | |
| TR | NVS_TR_gDAT | | | | | | | | | | | | | | 21.3 | | 8.1 | |
| | NVS_TR_hDAT | 0.17 | 11.2 | 2.3 | 0.23 | | | | | | | | | | 11.5 | | 8. | 11.3 |
| | NVS_TR_hNET | | 3.3 | 15.7 | | | | | | | | | | | | | 5.32 | |
| | NVS_TR_hSERT | | | | | | | | | | | | | | | | 2.4 | |
| | NVS_TR_rSERT | | | | | | | | | | | | | | | | 4.2 | |
| | NVS_TR_hAdoT | | | | | | | | | | | | | | | | 10.9 | |
| | NVS_TR_rVMAT2 | | 16.7 | 16.7 | | | | | | | | | | | | | 12.9 | |
| | TOX21_TR_LUC_GH3_Agonist | | | | | | | | | | | | | | | | | 0.23 |
| | TOX21_TR_LUC_GH3_Antagonist | | 58.6 | 59.2 | | 44.7 | | | | 0.046 | 86.5 | | 68.1 | | 33.8 | 47.3 | 40.3 | 75.1 |
| | TOX21_TR_LUC_GH3_Agonist_Followup | | | | | | | | | | | | | | | | | 1.2 |
| | TOX21_TR_RXR_BLA_Agonist_Followup_ratio[1] | | | | | | | | | | | | | | | | | 0.79 |
| | NVS_NR_hTRa_Antagonist | | | | | | | | | | | | | | | 14.6 | 7.5 | |
| | TOX21_TRB_BLA_Agonist_Followup_ch2 | | | | | | | | | | | | | | | | | 1.4 |
| | TOX21_TRB_BLA_Agonist_Followup_ratio | | | | | | | | | | | | | | | | | 1.5 |
| PPAR | ATG_PPARa_TRANS_up | | | | | | | | | | 58.9 | | | | | | | 76.8 |
| | ATG_PPARd_TRANS_up | | | | | | | | | | | | | | | | | 59.2 |
| | TOX21_PPARd_BLA_agonist_ratio | | | | | | | | | 0.44 | | | | | 91 | | | |
| | TOX21_PPARd_BLA_Antagonist_ch2 | | | 72.3 | | | | | | 0.026 | | | | | | | | |
| | TOX21_PPARd_BLA_antagonist_ratio | | 46.5 | 60.7 | | | | | | 0.027 | | | | | | | | |
| | ATG_PPARg_TRANS_up | | 46.4 | | 31.5 | 60.9 | | | | | 26.7 | | 122 | | | 21 | | 25.1 |
| | TOX21_PPARg_BLA_Agonist_ch2 | | | | | | | | | 0.026 | | | | | | | | 0.83 |
| | TOX21_PPARg_BLA_Agonist_ratio | | | | | | | | | | | | | | | | | 0.17 |
| | TOX21_PPARg_BLA_antagonist_ratio | | | | | | | | | 14.5 | | | | | | | | 55.1 |
| | NVS_NR_hPPARg | | | | | | | | | | 5.9 | | | | | | | |
| hdac | NVS_ENZ_hHDAC3_Activator | | | | | | | | | | | 1.1 | | | | | | |
| | NVS_ENZ_hHDAC3 | | | | | | | | | | 9.92 | | 0.094 | | | | | |
| | TOX21_HDAC_Inhibition | | | | | | | | | 11.1 | | | 49.3 | | | | | |
| | cytotoxicity | 8.9 | 9.9 | 11.4 | 6.2 | 14.3 | 0.05 | 1.6 | 1000 | 0.09 | 8.7 | 1000 | 7.9 | 1000 | 9.7 | 9.8 | 9.6 | 8.7 |

Targets correspond to those in Fig. 1; not all key targets (*e.g. cyp26*) were available in the ToxCast database. The second column shows the available assays for each respective target; values in the Table are AC50s (µM), shaded values are below cytotoxicity. No data: not tested. Cytotoxicity is the median of a range of assays (µM) in ToxCast. [1]Assay TOX21_TR_RXR_BLA_Agonist_Followup_ratio1 occurs under RXR and TR.

Table 5B – Summary activities in ToxCast assays per compound class or compound

| | |
|---|---|
| triazoles | RAR ≈ TR (not PPAR) |

| | | |
|---|---|---|
| AM580 | RAR (>) RXR | |
| TCDD | AhR | Rest not tested |
| dithiocarbamates | *RAR* | |
| thiram | PPARδ/γ > TR >[*RAR* ≈ *HDAC*] | |
| VPA | HDAC >> RXR | |
| PFOS | RAR ≈ PPARγ(α) | PPARδ not tested |
| | | |
| 2,4-dinitrophenol | HDAC>RAR>*AhR* | |
| boric acid | RXR | Rest not tested |
| endosulfan | *TR* > *RAR*/*RXR* | |
| Fenpropimorph | *AhR* ≈ *TR* ≈ *PPAR*γ ≈ *RXR* | |
| Prochloraz | AhR > RAR ≈ TR | |
| PCB126 | | not tested |
| RA | RXR > TR > RAR > PPARγ | |

*Italics*, AC50 above-median cytotoxicity

### *3.4 Molecular modeling*

The in silico molecular docking analysis was started with a restrictive binding energy analysis, which covered a wide range of isoforms of each target (Table S4). This initial analysis was followed by a more comprehensive method for a sub-selection of target proteins, and although there were some specific deviations among the two levels of analysis, the overall picture was similar. The results from the molecular modeling exercise (Table 6 and S4) indicate that triazoles are not selective for Cyp26 isoforms and can be classified as binders since they have low micromolar $K_i$ values. In fact, their binding affinity appears moderate compared to other reference and test compounds such as RA (ΔG ~ -8.6 kcal/mol; Ki ~ 10 µM). AM580 and CD3254, selective ligands for RAR (ΔG ~ -11 kcal/mol; Ki ~ 1 nM) and RXR (ΔG ~ -10 kcal/mol; Ki ~ 0.1 nM respectively), show a higher affinity to RAR and RXR isoforms than RA, while the three chemicals have the same potency for Cyp26- (ΔG ~ -9 kcal/mol; Ki ~ 0.1 µM) and PPAR- (ΔG ~ -7.5 kcal/mol; Ki ~ 1 µM) isoforms. HDAC8 showed selective affinity for VPA and CD3254, in contrast with the AhR ligands TCDD and PCB 126. Similarly, PFOS, which is a PPAR activator, did not show selective affinity for either of the two tested PPAR isoforms, since the PPAR binding site is larger than that of other nuclear receptors and therefore less selective. Endosulfan is the best RXR_BB ligand (ΔG = -12.5 kcal/mol; Ki ~ 0.1 nM). In general, it is possible to define a chemical as a ligand if it has an affinity value below -6.5 kcal/mol [85], which corresponds to a Ki of ~ 0.1 µM, increasing affinity values result in weak ligands and eventually in non-ligands (e.g. affinity of -4 kcal/mol corresponds to a Ki of ~ 1 mM). For instance, Metam is only a weak ligand for RXRs, while boric acid cannot be considered as a ligand for any protein. These and further specific observations are discussed below, also in the light of the differential gene expression data.

Table 6 – Modelled binding affinities of reference- and test compounds to key receptors and enzymes

| | | Cyp26a1 | Cyp26b1 | RAR_AA | RAR_AB | RXR_AA | RXR_BB | Ahr_2 | PPAR_AA | PPAR_G | HDAC 8 |
|---|---|---|---|---|---|---|---|---|---|---|---|
| Triazoles | Cyproconazole | -7.7 | -7.5 | -7.3 | -7.1 | -7.3 | -7.9 | -8.5 | -7 | -7 | -6.1 |
| | Flusilazole | -7.9 | -7.3 | -9 | -8.2 | -7.7 | -8.9 | -8.4 | -7.3 | -7.1 | -6.1 |
| | Hexaconazole | -7.4 | -8.2 | -8.6 | -7.5 | -7.5 | -7.9 | -8.3 | -6.8 | -6.9 | -6 |
| | Triadimefon | -7.4 | -7.7 | -8.8 | -8 | -8 | -8 | -8.2 | -6.8 | -6.6 | -6 |
| RAR | AM580 | -9 | -9.2 | -12 | -11.4 | -9.9 | -10 | -9.7 | -7.3 | -7 | -7 |
| RXR | CD3254 | -9.1 | -8.5 | -11 | -10.4 | -9.7 | -10.5 | -10 | -7.1 | -7.2 | -12.6 |
| AhR | TCDD | -6.9 | -6.1 | -7.9 | -7.5 | -6.6 | -6.2 | -6.8 | -5.8 | -5.9 | -6.3 |
| HDAC | VPA | -6.2 | -5.8 | -6.1 | -5.5 | -6.3 | -6.9 | -6.1 | -5.4 | -5.6 | -10.9 |
| PPAR | PFOS | -6.7 | -6.6 | -7.8 | -6.6 | -7.5 | -8.4 | -7.7 | -6 | -6.1 | -5.5 |
| Dithio-carbamates | Maneb | -6.4 | -5.2 | -7.3 | -6.5 | -6.8 | -6.5 | -5.9 | -5.1 | -5.3 | -7.3 |
| | Metam | -4.3 | -3.9 | -4.7 | -4.6 | -5.3 | -5.3 | -4.3 | -3.8 | -3.9 | -3.6 |
| | Thiram | -6.5 | -6.3 | -7.5 | -6.8 | -6.7 | -6.9 | -6.4 | -5.7 | -5.9 | -5.9 |
| | 2,4-Dinitrophenol | -5.7 | -5.6 | -6.8 | -6.2 | -5.6 | -5.8 | -6.1 | -5.2 | -5.3 | -5.3 |
| | Boric Acid | -3.3 | -3.3 | -3.3 | -3.3 | -3.3 | -3.3 | -3.3 | -3.3 | -3.3 | -3.2 |
| | Endosulfan | -9.4 | -9.1 | -10.3 | -9 | -9.5 | -12.5 | -8.7 | -5.3 | -5.1 | -4.8 |
| | Fenpropimorph | -8.7 | -8.3 | -9 | -8 | -9.2 | -9.6 | -8.6 | -7.6 | -7.8 | -6.3 |
| | Prochloraz | -7.9 | -7.8 | -8.9 | -8 | -8.2 | -8.2 | -8.4 | -7.5 | -7.6 | -7.3 |
| | PCB126 | -7 | -6.3 | -6.8 | -6 | -6.7 | -6.8 | -6.9 | -5.7 | -5.7 | -5.8 |
| | RA | -8.9 | -8.6 | -9.8 | -10 | -9.5 | -10.1 | -8.9 | -7.5 | -7.5 | -6.7 |

Affinities are expressed as kcal/mol. Values are formatted applying -6.5 kcal/mol as a cut-off value for relevance.

## 4. Discussion

The basis for risk assessment of mixtures is an informed prediction of the toxicological hazard of the considered combination of chemical compounds. Following the EFSA CAG strategy for an achievable modeling of mixture effects [4], key information for each compound is its target organ or biological process (level 1), the specific phenotype of the effect (level 2), and knowledge about its mode and mechanism of action (level 3/4). The first two levels can be derived from toxicological test models, and are generally well available for compounds relevant for human exposure. However, information on MOA of compounds is generally scarce and complicated by the fact that many compounds have multiple MOAs (Table 3). This hampers an informed decision on (dis)similarities of MOAs in a mixture and thus the decision whether dose-addition could be a plausible way to model mixture effects.

Previously, we confirmed the EFSA assumption that in cumulative risk assessment dose-addition can be used as a default model to predict combination effects irrespective of MOA [7], in a variety of binary mixtures in a zebrafish embryo model for craniofacial malformations [8]. Yet, being able to test what MOA or which set of MOAs is activated may be crucial for understanding the effect of a compound on development. Also, whether or not the model of dose-addition can be used as default for more complex mixtures remains to be determined. Therefore, in this study, we analyzed an array of marker genes for differential gene expression in zebrafish embryos and the ensuing potential to distinguish MOAs. The array of marker genes was optimized in several rounds of experiments, excluding non-informative markers and adding new candidates. The final selection of genes could distinguish reference compound classes, associated with known or assumed MOAs, and marker profiles of test compounds could be matched with the reference MOAs through various grades of overlap.

To verify and substantiate these results, the potential of compounds to activate initial targets in the identified pathways was retrieved from the ToxCast database of *in vitro* activation assays. As a second approach, the same set of compounds was analyzed for modeled binding to key target molecules through *in silico* molecular docking.

### *4.1 Robustness of markers*

Generally, there was a good reproducibility of particularly informative marker genes within compound classes. However, exceptions for single markers or even a full experiment (see first PCB 126 in Table S3), can be understood from unintended experimental variations such as differences in exposure concentration, timing of start of exposure and termination of the experiment, or varying stages of development among batches of embryos. In general, the relative level of gene expression may depend on the relative responsiveness of a given pathway (within a cell), but can also be affected by the relative size of the population of responding cells within the whole embryo. Another factor is the critical response time windows. When these are narrow, this may produce critical response variations with limited shifts in timing of analysis of developmental stages. Finally, the studied compounds are probably active in a wider range of tissues than the developing head skeleton, which was the phenotypic anchor for the applied test concentrations, and the detected gene expression signals may thus not always inform about processes in the phenotypic anchoring tissue. Altogether the detected responses may be

affected by spatial and temporal dynamics of gene expression. This is obviously true for disruption of RA signalling, which has a delicately regulated role in time and space in a wide range of developmental processes [86]. This holds also for the case of dithiocarbamates, where the embryos show overall axial/notochord malformations in addition to the effects on the jawbones [12, 22]. Dose-responses in differential gene expression were not established, but since there was no difference between gene expression responses of the two tested TCDD concentrations (10 and 100 nM), dose-responses for gene expression and phenotype may be different. Although genetic variation between strains could be another factor, but this was not apparent as a source of bias in our experiments. The variation in size of the response between compound classes, e.g. for *hoxb1a* among AM580 (selectively RAR), triazoles, and RA, may indicate the relative specificity of the respective compounds to regulate such a downstream marker in a dedicated pathway.

*4.2 Functional position of markers in pathways, specificity of responses*

When comparing observed responses in differential gene expression (Table 4B) with anticipated responses (Fig. 1), the effect of triazoles on *cyp26* genes is strongly confirmed. This is also true for the downstream genes *igfbp*, *hoxb1a*, *lhx8a*, but not so much for *dlx5a*. These markers, which are all informative of a disbalance in RA concentrations, are thus functionally related to effects on RA regulated normal development of the head skeleton [30]. An additional response with triazoles was observed in *loxl3b*, this is possibly associated with *sox9a* downregulation. Downregulation of *loxl3b* related to RA signalling was further confirmed by a similar effect after exposure to RA and to the pure RAR and RXR agonists AM580 and CD3254. This is in line with the established general but pivotal role of lysyl oxidases in notochord development [87], and in particular with the functional role of *loxl3* in craniofacial development in zebrafish [88] and in mice [89]. RA has been reported to regulate expression in the lysyl oxidase-like family, albeit in the context of other biological systems such as wound healing and adipocyte differentiation [90, 91]. The pure RAR and RXR agonists AM580 and CD3254 both also induced upregulation of c*yp26a1*, like triazoles, but in contrast, downregulation of c*yp26b1*, and these two compounds further showed both overlapping and contrasting responses. The ToxCast data, however, tone down the RAR specificity of AM580, in view of similar activity in one RXR assay (Table 5A, B). The differences between triazoles and either of the RAR or RXR profiles suggest that other MOAs contributed to the triazole profile, which can be understood from the overview in Table 3, and is also supported by TR activity of triazoles in ToxCast assays (Table 5 A, B). Interestingly, ToxCast data also confirmed the activity of RA on TR and PPARγ in addition to RAR/RXR, possibly explaining the incomplete match with either of the RAR or RXR profiles.

It is known that dithiocarbamates produce severe craniofacial malformations in zebrafish embryos [8, 12, 51]. However, the initially included marker *loxl3b*, which was identified by van Boxtel *et al.* [51] , was not regulated by DTCs in our qPCR analysis. This may be due to a limited overall expression level, which is detectable by the tissue-specific *in situ* hybridization applied by van Boxtel *et al.* [88] but remains undetected by qPCR in the noise of the whole embryo mRNA extract. The timing of differential gene expression analysis (72hpf in this study vs versus 48hpf in the van Boxtel *et al.* study) may be an additional factor.

Of the markers *myod*, *ntla* and *col2a* [23], only *ntla* was regulated by the applied dithiocarbamates, but not in a distinctive manner given the similar upregulation by VPA. Therefore, an upstream regulator of *ntla*, *nf-kb* (*rela*) [92], which is reported to be inhibited by dithiocarbamates [93], was added. However, similar to *loxl3b*, no regulation of the anticipated response in *rela* was observed. On the other hand, *rela* was upregulated by VPA, whereas endosulfan and fenpropimorph induced downregulation of *rela* (and upregulation of *ntla*), thereby better representing the anticipated dithiocarbamate profile than the carbamates themselves. Only two predicted responses for dithiocarbamates were confirmed, i.e. *sox9b* and *ntla.* Further responses with these compounds in *hoxb1* and *dhfr* can be understood via the oxidative stress and *sox* pathways. The observed responses in *igfbp*, *cpt1b*, *aclya*, and *hmgcra* may be associated with activation of PPAR, thyroid receptor (TR), and, with lower certainty RAR and HDAC. In particular RAR and HDAC activation are also reported in the ToxCast database although only for thiram, with limited to no relevant data available for respectively maneb and metam.

The key response of *sox9b* with TCDD *via* AhR was indeed anticipated (Fig. 1), as was a response in *igfbp.* Responses of TCDD downstream of RA regulation (*cyp26* genes, *lhx8a*) have a possible link *via* an effect on RA metabolism.

The dominating response after VPA exposure was reduced expression of *cpt1b,* which was anticipated through the interaction of VPA with coenzyme-A (CoA; Fig. 1). Also, the upregulation of *hoxb1a* was anticipated, whereas another downregulated expression was expected in *lhx8a*. *Aclya*, a target of PPARα, was selectively upregulated by VPA. Although VPA can also directly activate PPARs [44], this may not be a primary pathway in view of the absence of *aclya* response with PFOS. No data on PPAR assays tested with VPA were reported in ToxCast. Alternatively, VPA may cut an endogenous source of acetate for synthesis of acetyl-CoA through HDAC inhibition and acss1/2 [94], possibly followed by activation of the synthesis route *via aclya*. This process could be enhanced by a further HDAC inhibiting effect of excess unconjugated CoA [95].

In contrast to VPA, PFOS induced a remarkable upregulation of *cpt1b*, accompanied by relatively strong upregulation of *igfbp* and downregulation of *sox9b,* both reminiscent to dioxin-like effects. The anticipated effects on expression of *dhfr* and *hmgcra* (but not *aclya*) were confirmed. ToxCast data confirmed PPAR activation with PFOS (although at a similar level as activation of RAR), whereas no data was available on activity of PFOS in AhR assays.

Table 7 – Comparison of test compound activities across assays

| reference compound / target | 2,4-dinitrophenol | | | Boric Acid | | | Endosulfan | | | Fenpropimorph | | | Prochloraz | | | PCB126 | | | RA | | |
|---|---|---|---|---|---|---|---|---|---|---|---|---|---|---|---|---|---|---|---|---|---|
| | DGE | TC | BA | DGE | TC | BA | DGE | TC | BA | DGE | TC | BA | DGE | TC | BA | DGE | TC | BA | DGE | TC | BA |
| 3AZ / Cyp26 | - | 0 | - | ± | 0 | - | - | 0 | ++ | ± | 0 | ++ | - | 0 | + | - | 0 | ± | - | 0 | + |
| AM580 / RAR | + | ++ | + | ++ | 0 | - | - | [+] | ++ | ± | 0 | ++ | ± | + | ++ | ± | 0 | ± | + | + | ++ |
| CD3254 / RXR | - | 0 | - | - | ++ | - | ± | [+] | +++ | ± | [+] | ++ | - | - | ++ | - | 0 | ± | - | +++ | ++ |
| DL / AhR | ++ | [+] | ± | - | 0 | - | - | 0 | ++ | - | [+] | ++ | - | ++ | ++ | ++ | 0 | ± | - | 0 | ++ |
| DTC | ± | 0 | 0 | ± | 0 | 0 | ± | 0 | 0 | + | 0 | 0 | ± | 0 | 0 | ± | 0 | 0 | - | 0 | 0 |
| VPA / HDAC | - | +++ | - | ± | 0 | - | - | 0 | - | - | 0 | - | - | 0 | ++ | ± | 0 | - | - | 0 | + |
| PFOS / PPAR | ± | - | - | - | 0 | - | ++ | - | - | ± | ++ | - | ± | 0 | ++ | ± | 0 | - | - | ± | ± |
| TR | 0 | - | 0 | 0 | 0 | 0 | 0 | [++] | 0 | 0 | [+] | 0 | 0 | + | 0 | 0 | 0 | 0 | 0 | ++ | 0 |

DGE, differential gene expression profile; TC, activity in ToxCast assays; BA, binding affinity. Number of +s is an approximate indication of relative strength of activity in the respective models, with -, no activity; square brackets, activity below cytotoxicity limit; 0, not tested. Green and red cells indicate match (green) and no match (red) of ToxCast activity and binding affinity with DGE profiles.

*4.3 Complex profiles of test compounds*

Although the final set of marker genes was selected to reflect the known predominant MOA of each reference compound class, additional activities were also observed with these compounds. In profiles obtained with most test compounds, no single full and exact match was observed with one of the reference compounds. Instead, less MOA specificity, or more complex actions as compared to reference compounds, was apparent, probably relating to activation of multiple targets and downstream pathways by compounds. Similarly, pleiotropic activities of the test compounds were seen in the outcome of the ToxCast assays, as far as compounds were tested (Table 5B, bottom set). Overall, a pleiotropic activity will result in a complex marker gene profile, although a single MOA can still dominate the activation pattern. Thus, boric acid, endosulfan, fenpropimorph, PCB126, and RA all showed predominating matches with respectively the profiles of AM580, PFOS, dithiocarbamates, TCDD, and triazoles/AM580, while a clear dual match was observed for 2.4-dinitrophenol, with dioxin-like and AM580 profiles. Prochloraz could not be mapped to any of the profiles (Table 4C). In approximately half of the cases, matches with positive or negative gene expression were confirmed by either ToxCast activities or binding affinity analysis (Table 7). This seemingly poor concordance can be partly explained by either limited overlap of assays (e.g. key MOAs RAR for boric acid and AhR for PCB126 were not tested in ToxCast), or limitations to performance of assays. In this respect, boric acid did not show binding affinity for any of the analyzed targets, possibly related to an intrinsic technical issue hampering *in silico* modeling for this molecule. Since the affinity values (Table 6) provide quantitative information on the strength of binding, this information was used to prioritize chemicals and to discriminate preferential

targets for each chemical among the selected proteins. All these data are meant to support gene expression profile observations (Table 4 A-C). However, neither the evaluation of intrinsic activities on nuclear receptors nor the classification as substrate/inhibitor on enzymes can be made on the basis of the affinity values of a chemical and the conclusive potential *per se* is therefore limited. To enhance this, further (demanding) in silico approaches would have to be applied which are currently only possible for hormone nuclear receptors [85, 96]. Vice versa, ToxCast assays also detected activities, which were to some extent confirmed by binding affinity analysis but not reflected in the gene expression profiles. Some obvious examples are activity and binding of RA to RXR, interaction between AhR and prochloraz, and limited binding affinity for AhR of the well-known AhR activator TCDD. These examples can likely be explained through characteristics of the zebrafish embryo model, i.e. loss of specific signal from a small population of cells in the whole embryo, developmental stage-dependent expression, or alternatively, limited penetration of the initial activation in the downstream pathway indicating that further testing and validation is required for all three types of assays

*4.4 Conclusion*

In conclusion, the differential gene expression analysis presented in this paper demonstrates that the selected set of marker genes can provide information on the MOA of a compound, in this case relating to craniofacial skeletal development. Understanding the MOA or complex of MOAs of compounds is important to distinguish similar and dissimilar MOAs for dose-response modelling in combined exposures. Since marker genes may play a role in several pathways, and *vice versa,* compounds may be active in multiple pathways. Therefore, the activation/repression profile of the applied limited (but well-chosen) qPCR array will not per se in all cases identify specific MOAs but can be applied as a practical tool to weigh overlap between compounds and thus evaluate (dis)similarity of MOAs of compounds in mixtures. The ToxCast *in vitro* target activity and the *in silico* binding affinity analysis are helpful to confirm and understand MOAs suggested by differential gene expression analysis in the zebrafish. *Vice versa*, these *in vitro* and *in silico* tools could be useful as an alternative screen and direct further hypothesis formulation and experimental analysis. In the end, a combination of such alternative tools can inform MOA models and in combination build evidence for particular MOAs such as craniofacial malformation in zebrafish embryos for which disrupted RA-signalling provides a key MOA. While comprising several different compounds with known as well as unknown MOAs, the data presented in this paper suggest that in mixture analysis, a complex MOA will generally be a valid assumption, and similar MOA can probably only be observed in compounds that are chemically closely related. Consequently, It is likely that these conclusions also apply to CAGs or endpoints other than craniofacial skeletal development.

**Declaration of interests**

The authors declare that they have no known competing financial interests or personal relationships that could have appeared to influence the work reported in this paper.

**Acknowledgments**

This work was part of the H2020-project EuroMix - WP3: Bioassay toolbox and mixture testing (www.euromixproject.eu), which was funded by the European Commission (Grant Agreement 633172), and by the Dutch Ministry of Health, Welfare and Sports (VWS) (project 5.1.2: Knowledgebase and policy advise on CMRS substances). LP and IE were supported by grants from MIUR – Progetto Eccellenza. IE was supported by FFABR 2017 and a Departmental "Linea 2-2019" grant. Shalenie den Braver-Sewradj and Yvonne Staal are acknowledged for reviewing the draft manuscript.

**References**

[1] S. Rotter, A. Beronius, A.R. Boobis, A. Hanberg, J. van Klaveren, M. Luijten, K. Machera, D. Nikolopoulou, H. van der Voet, J. Zilliacus, R. Solecki, Overview on legislation and scientific approaches for risk assessment of combined exposure to multiple chemicals: the potential EuroMix contribution, Critical reviews in toxicology 48(9) (2018) 796-814.
[2] A.R. Boobis, B.C. Ossendorp, U. Banasiak, P.Y. Hamey, I. Sebestyen, A. Moretto, Cumulative risk assessment of pesticide residues in food, Toxicol Lett 180(2) (2008) 137-50.
[3] T. Colnot, W. Dekant, Approaches for grouping of pesticides into cumulative assessment groups for risk assessment of pesticide residues in food, Regulatory toxicology and pharmacology : RTP 83 (2017) 89-99.
[4] P.o.P.P.P.a.t.R.P. EFSA, Scientific Opinion on the identification of pesticides to be included in cumulative assessment groups on the basis of their toxicological profile, EFSA Journal 11(7) (2013) 131.
[5] E. Nielsen, Nørhede, P., Boberg, J., Krag Isling, L., Kroghsbo, S., Hadrup, N., Bredsdorff, L., Mortensen, A., Christian Larsen, J., Identification of Cumulative Assessment Groups of Pesticides, EFSA Supporting Publications 9(4) (2012).
[6] A.F. Hernandez, F. Gil, M. Lacasana, Toxicological interactions of pesticide mixtures: an update, Archives of toxicology 91(10) (2017) 3211-3223.
[7] EFSA-PPR-Panel, Scientific Opinion on relevance of dissimilar mode of action and its appropriate application for cumulative risk assessment of pesticides residues in food, EFSA Journal 11(12) (2013) 3472-3512.
[8] M. Zoupa, E.P. Zwart, E.R. Gremmer, A. Nugraha, S. Compeer, W. Slob, L.T.M. van der Ven, Dose addition in chemical mixtures inducing craniofacial malformations in zebrafish (*Danio rerio*) embryos, Food Chem Toxicol 137 (2020) 111117.
[9] B.D. Abbott, L.S. Birnbaum, TCDD-induced altered expression of growth factors may have a role in producing cleft palate and enhancing the incidence of clefts after coadministration of retinoic acid and TCDD, Toxicology and applied pharmacology 106(3) (1990) 418-32.
[10] G.R. Garcia, S.M. Bugel, L. Truong, S. Spagnoli, R.L. Tanguay, AHR2 required for normal behavioral responses and proper development of the skeletal and reproductive systems in zebrafish, PloS one 13(3) (2018) e0193484.
[11] J.P. Souder, D.A. Gorelick, ahr2, But Not ahr1a or ahr1b, Is Required for Craniofacial and Fin Development and TCDD-dependent Cardiotoxicity in Zebrafish, Toxicological sciences : an official journal of the Society of Toxicology 170(1) (2019) 25-44.

[12] Y.C.M. Staal, J. Meijer, R.J.C. van der Kris, A.C. de Bruijn, A.Y. Boersma, E.R. Gremmer, E.P. Zwart, P.K. Beekhof, W. Slob, L.T.M. van der Ven, Head skeleton malformations in zebrafish (Danio rerio) to assess adverse effects of mixtures of compounds, Archives of toxicology 92(12) (2018) 3549-3564.
[13] F. Di Renzo, M.L. Broccia, E. Giavini, E. Menegola, Stage-dependent abnormalities induced by the fungicide triadimefon in the mouse, Reproductive toxicology (Elmsford, N.Y.) 31(2) (2011) 194-9.
[14] E.C. Tonk, J.L. Pennings, A.H. Piersma, An adverse outcome pathway framework for neural tube and axial defects mediated by modulation of retinoic acid homeostasis, Reproductive toxicology (Elmsford, N.Y.) 55 (2015) 104-13.
[15] M.S. Hutson, M.C.K. Leung, N.C. Baker, R.M. Spencer, T.B. Knudsen, Computational Model of Secondary Palate Fusion and Disruption, Chem Res Toxicol 30(4) (2017) 965-979.
[16] Y.L. Yan, C.T. Miller, R.M. Nissen, A. Singer, D. Liu, A. Kirn, B. Draper, J. Willoughby, P.A. Morcos, A. Amsterdam, B.C. Chung, M. Westerfield, P. Haffter, N. Hopkins, C. Kimmel, J.H. Postlethwait, A zebrafish sox9 gene required for cartilage morphogenesis, Development 129(21) (2002) 5065-79.
[17] K.M. Xiong, R.E. Peterson, W. Heideman, Aryl hydrocarbon receptor-mediated down-regulation of sox9b causes jaw malformation in zebrafish embryos, Mol Pharmacol 74(6) (2008) 1544-53.
[18] K. Fathe, A. Palacios, R.H. Finnell, Brief report novel mechanism for valproate-induced teratogenicity, Birth Defects Res A Clin Mol Teratol 100(8) (2014) 592-7.
[19] M. Haberland, M.H. Mokalled, R.L. Montgomery, E.N. Olson, Epigenetic control of skull morphogenesis by histone deacetylase 8, Genes Dev 23(14) (2009) 1625-30.
[20] S.E. Wahl, A.E. Kennedy, B.H. Wyatt, A.D. Moore, D.E. Pridgen, A.M. Cherry, C.B. Mavila, A.J. Dickinson, The role of folate metabolism in orofacial development and clefting, Developmental biology 405(1) (2015) 108-22.
[21] K.A. Lloyd, A scientific review: mechanisms of valproate-mediated teratogenesis, Bioscience Horizons 6 (2013) 1-10.
[22] A.L. van Boxtel, J.H. Kamstra, D.M. Fluitsma, J. Legler, Dithiocarbamates are teratogenic to developing zebrafish through inhibition of lysyl oxidase activity, Toxicology and applied pharmacology 244(2) (2010) 156-61.
[23] F. Tilton, J.K. La Du, M. Vue, N. Alzarban, R.L. Tanguay, Dithiocarbamates have a common toxic effect on zebrafish body axis formation, Toxicology and applied pharmacology 216(1) (2006) 55-68.
[24] A.L. Van Boxtel, Kamstra, J. H., Fluitsma, D. M., Legler, J., Dithiocarbamates are teratogenic to developing zebrafish through inhibition of lysyloxidase activity, Toxicology and Applied Pharmacology 244(2) (2010) 156-161.
[25] S. Era, K.H. Harada, M. Toyoshima, K. Inoue, M. Minata, N. Saito, T. Takigawa, K. Shiota, A. Koizumi, Cleft palate caused by perfluorooctane sulfonate is caused mainly by extrinsic factors, Toxicology 256(1-2) (2009) 42-7.
[26] R. Martinez, L. Herrero-Nogareda, M. Van Antro, M.P. Campos, M. Casado, C. Barata, B. Pina, L. Navarro-Martin, Morphometric signatures of exposure to endocrine disrupting chemicals in zebrafish eleutheroembryos, Aquatic toxicology (Amsterdam, Netherlands) 214 (2019) 105232.
[27] C.E. Jantzen, K.A. Annunziato, S.M. Bugel, K.R. Cooper, PFOS, PFNA, and PFOA sub-lethal exposure to embryonic zebrafish have different toxicity profiles in terms of morphometrics, behavior and gene expression, Aquatic toxicology (Amsterdam, Netherlands) 175 (2016) 160-70.
[28] C. Lau, K. Anitole, C. Hodes, D. Lai, A. Pfahles-Hutchens, J. Seed, Perfluoroalkyl acids: a review of monitoring and toxicological findings, Toxicological sciences : an official journal of the Society of Toxicology 99(2) (2007) 366-94.
[29] M.B. Rosen, K.P. Das, J. Rooney, B. Abbott, C. Lau, J.C. Corton, PPARalpha-independent transcriptional targets of perfluoroalkyl acids revealed by transcript profiling, Toxicology 387 (2017) 95-107.

[30] E. Menegola, M.L. Broccia, F. Di Renzo, E. Giavini, Postulated pathogenic pathway in triazole fungicide induced dysmorphogenic effects, Reproductive toxicology (Elmsford, N.Y.) 22(2) (2006) 186-95.
[31] M. Dimopoulou, A. Verhoef, J.L.A. Pennings, B. van Ravenzwaay, I.M.C.M. Rietjens, A.H. Piersma, Embryotoxic and pharmacologic potency ranking of six azoles in the rat whole embryo culture by morphological and transcriptomic analysis, Toxicology and applied pharmacology 322 (2017) 15-26.
[32] S. Hester, T. Moore, W.T. Padgett, L. Murphy, C.E. Wood, S. Nesnow, The hepatocarcinogenic conazoles: cyproconazole, epoxiconazole, and propiconazole induce a common set of toxicological and transcriptional responses, Toxicological sciences : an official journal of the Society of Toxicology 127(1) (2012) 54-65.
[33] R.C. Peffer, J.G. Moggs, T. Pastoor, R.A. Currie, J. Wright, G. Milburn, F. Waechter, I. Rusyn, Mouse liver effects of cyproconazole, a triazole fungicide: role of the constitutive androstane receptor, Toxicological sciences : an official journal of the Society of Toxicology 99(1) (2007) 315-25.
[34] J. Jiang, G. Hu, C. Zhang, X. Zhao, Q. Wang, L. Chen, Toxicological analysis of triadimefon on endocrine disruption and oxidative stress during rare minnow (Gobiocypris rarus) larvae development, Environmental science and pollution research international 24(34) (2017) 26681-26691.
[35] W. Zhang, L. Chen, Y. Xu, Y. Deng, L. Zhang, Y. Qin, Z. Wang, R. Liu, Z. Zhou, J. Diao, Amphibian (Rana nigromaculata)exposed to cyproconazole: Changes in growth index, behavioral endpoints, antioxidant biomarkers, thyroid and gonad development, Aquatic toxicology (Amsterdam, Netherlands) 208 (2019) 62-70.
[36] H.J. Heusinkveld, J. Molendijk, M. van den Berg, R.H. Westerink, Azole fungicides disturb intracellular Ca2+ in an additive manner in dopaminergic PC12 cells, Toxicological sciences : an official journal of the Society of Toxicology 134(2) (2013) 374-81.
[37] S. Liu, J. Chang, Y. Zhao, G. Zhu, Changes of thyroid hormone levels and related gene expression in zebrafish on early life stage exposure to triadimefon, Environmental toxicology and pharmacology 32(3) (2011) 472-7.
[38] D.C. Wolf, J.W. Allen, M.H. George, S.D. Hester, G. Sun, T. Moore, S.F. Thai, D. Delker, E. Winkfield, S. Leavitt, G. Nelson, B.C. Roop, C. Jones, J. Thibodeaux, S. Nesnow, Toxicity profiles in rats treated with tumorigenic and nontumorigenic triazole conazole fungicides: Propiconazole, triadimefon, and myclobutanil, Toxicol Pathol 34(7) (2006) 895-902.
[39] H. Kagechika, Novel synthetic retinoids and separation of the pleiotropic retinoidal activities, Curr Med Chem 9(5) (2002) 591-608.
[40] P.W. Jurutka, I. Kaneko, J. Yang, J.S. Bhogal, J.C. Swierski, C.R. Tabacaru, L.A. Montano, C.C. Huynh, R.A. Jama, R.D. Mahelona, J.T. Sarnowski, L.M. Marcus, A. Quezada, B. Lemming, M.A. Tedesco, A.J. Fischer, S.A. Mohamed, J.W. Ziller, N. Ma, G.M. Gray, A. van der Vaart, P.A. Marshall, C.E. Wagner, Modeling, synthesis, and biological evaluation of potential retinoid X receptor (RXR) selective agonists: novel analogues of 4-[1-(3,5,5,8,8-pentamethyl-5,6,7,8-tetrahydro-2-naphthyl)ethynyl]benzoic acid (bexarotene) and (E)-3-(3-(1,2,3,4-tetrahydro-1,1,4,4,6-pentamethylnaphthalen-7-yl)-4-hydroxypheny l)acrylic acid (CD3254), J Med Chem 56(21) (2013) 8432-54.
[41] H. Liu, F.H. Nie, H.Y. Lin, Y. Ma, X.H. Ju, J.J. Chen, R. Gooneratne, Developmental toxicity, EROD, and CYP1A mRNA expression in zebrafish embryos exposed to dioxin-like PCB126, Environ Toxicol 31(2) (2016) 201-10.
[42] H. Liu, F.H. Nie, H.Y. Lin, Y. Ma, X.H. Ju, J.J. Chen, R. Gooneratne, Developmental toxicity, oxidative stress, and related gene expression induced by dioxin-like PCB 126 in zebrafish (Danio rerio), Environ Toxicol 31(3) (2016) 295-303.
[43] A. Lampen, M. Gottlicher, H. Nau, Prediction of embryotoxic effects of valproic acid-derivatives with molecular in vitro methods, ALTEX 18(2) (2001) 123-6.

[44] E. Szalowska, B. van der Burg, H.Y. Man, P.J. Hendriksen, A.A. Peijnenburg, Model steatogenic compounds (amiodarone, valproic acid, and tetracycline) alter lipid metabolism by different mechanisms in mouse liver slices, PloS one 9(1) (2014) e86795.
[45] C.M. Chuang, C.H. Chang, H.E. Wang, K.C. Chen, C.C. Peng, C.L. Hsieh, R.Y. Peng, Valproic acid downregulates RBP4 and elicits hypervitaminosis A-teratogenesis--a kinetic analysis on retinol/retinoic acid homeostatic system, PloS one 7(9) (2012) e43692.
[46] K.P. Das, B.E. Grey, M.B. Rosen, C.R. Wood, K.R. Tatum-Gibbs, R.D. Zehr, M.J. Strynar, A.B. Lindstrom, C. Lau, Developmental toxicity of perfluorononanoic acid in mice, Reproductive toxicology (Elmsford, N.Y.) 51 (2015) 133-44.
[47] X. Shi, Y. Du, P.K. Lam, R.S. Wu, B. Zhou, Developmental toxicity and alteration of gene expression in zebrafish embryos exposed to PFOS, Toxicology and applied pharmacology 230(1) (2008) 23-32.
[48] X. Shi, C. Liu, G. Wu, B. Zhou, Waterborne exposure to PFOS causes disruption of the hypothalamus-pituitary-thyroid axis in zebrafish larvae, Chemosphere 77(7) (2009) 1010-8.
[49] K.S. Larsson, C. Arnander, E. Cekanova, M. Kjellberg, Studies of teratogenic effects of the dithiocarbamates maneb, mancozeb, and propineb, Teratology 14(2) (1976) 171-83.
[50] I. Hajdu, J. Kardos, B. Major, G. Fabo, Z. Lorincz, S. Cseh, G. Dorman, Inhibition of the LOX enzyme family members with old and new ligands. Selectivity analysis revisited, Bioorganic & medicinal chemistry letters 28(18) (2018) 3113-3118.
[51] A.L. van Boxtel, B. Pieterse, P. Cenijn, J.H. Kamstra, A. Brouwer, W. van Wieringen, J. de Boer, J. Legler, Dithiocarbamates induce craniofacial abnormalities and downregulate sox9a during zebrafish development, Toxicological sciences : an official journal of the Society of Toxicology 117(1) (2010) 209-17.
[52] J. Zhang, Z. Liu, T. Zhang, Z. Lin, Z. Li, A. Zhang, X. Sun, J. Gao, Loss of Lysyl Oxidase-like 3 Attenuates Embryonic Lung Development in Mice, Scientific reports 6 (2016) 33856.
[53] X. Chen, M. Fang, M. Chernick, F. Wang, J. Yang, Y. Yu, N. Zheng, H. Teraoka, S. Nanba, T. Hiraga, D.E. Hinton, W. Dong, The case for thyroid disruption in early life stage exposures to thiram in zebrafish (Danio rerio), General and comparative endocrinology 271 (2019) 73-81.
[54] C.L. Hsieh, K.C. Chen, P.X. Lin, C.C. Peng, R.Y. Peng, Resveratrol and vitamin E rescue valproic acid-induced teratogenicity: the mechanism of action, Clin Exp Pharmacol Physiol 41(3) (2014) 210-9.
[55] A.M. Quintana, J.A. Hernandez, C.G. Gonzalez, Functional analysis of the zebrafish ortholog of HMGCS1 reveals independent functions for cholesterol and isoprenoids in craniofacial development, PloS one 12(7) (2017) e0180856.
[56] R. Keber, H. Motaln, K.D. Wagner, N. Debeljak, M. Rassoulzadegan, J. Acimovic, D. Rozman, S. Horvat, Mouse knockout of the cholesterogenic cytochrome P450 lanosterol 14alpha-demethylase (Cyp51) resembles Antley-Bixler syndrome, J Biol Chem 286(33) (2011) 29086-97.
[57] M.A. Tucker, F. Lopez-Ruiz, H.J. Cools, J.G.L. Mullins, K. Jayasena, R.P. Oliver, Analysis of mutations in West Australian populations of Blumeria graminis f. sp. Hordei CYP51 conferring resistance to DMI fungicides, Pest Manag Sci (2019).
[58] A.M. Morrison, J.V. Goldstone, D.C. Lamb, A. Kubota, B. Lemaire, J.J. Stegeman, Identification, modeling and ligand affinity of early deuterostome CYP51s, and functional characterization of recombinant zebrafish sterol 14alpha-demethylase, Biochim Biophys Acta 1840(6) (2014) 1825-36.
[59] P. Marx-Stoelting, K. Ganzenberg, C. Knebel, F. Schmidt, S. Rieke, H. Hammer, F. Schmidt, O. Potz, M. Schwarz, A. Braeuning, Hepatotoxic effects of cyproconazole and prochloraz in wild-type and hCAR/hPXR mice, Archives of toxicology 91(8) (2017) 2895-2907.
[60] A.K. Goetz, D.J. Dix, Mode of action for reproductive and hepatic toxicity inferred from a genomic study of triazole antifungals, Toxicological sciences : an official journal of the Society of Toxicology 110(2) (2009) 449-62.

[61] I.L. Leong, T.Y. Tsai, K.L. Wong, L.R. Shiao, K.S. Cheng, P. Chan, Y.M. Leung, Valproic acid inhibits ATP-triggered Ca(2+) release via a p38-dependent mechanism in bEND.3 endothelial cells, Fundam Clin Pharmacol 32(5) (2018) 499-506.
[62] T.D. Schmittgen, K.J. Livak, Analyzing real-time PCR data by the comparative CT method, Nature Protocols 3(6) (2008) 1101-1108.
[63] S.A. Hermsen, T.E. Pronk, E.J. van den Brandhof, L.T. van der Ven, A.H. Piersma, Triazole-induced gene expression changes in the zebrafish embryo, Reproductive toxicology (Elmsford, N.Y.) 34(2) (2012) 216-24.
[64] M. Abe, Wakisaka, T.,, Retinoic acid affects craniofacial patterning by changing Fgf8 expression in the pharyngeal ectoderm, Development, growth and differentiation 50(9) (2008) 717-729.
[65] T. Shimomura, Kawakami, M., Okuda, H., Tatsumi, K., Morita, S., Nochioka, K., Kirita, T., Wanaka, A., Retinoic acid regulates Lhx8 expression via FGF-8b to the upper jaw development of chick embryo., Journal of Bioscience and Bioengineering 119(3) (2015) 260-266.
[66] N. Funato, Nakumura, M., Identification of shared and unique gene families associated with oral clefts, International Journal of Oral Science 9(2) (2017) 104-109.
[67] S.M. Hutson, Leung, M. C. K., Baker, N. C. Spencer, R. M., Knudsen, T. B., Computational Model of Secondary Palate Fusion and Disruption, Chemical Researcj om Toxicology 30(4) (2017) 965-979.
[68] T. Shimomura, M. Kawakami, H. Okuda, K. Tatsumi, S. Morita, K. Nochioka, T. Kirita, A. Wanaka, Retinoic acid regulates Lhx8 expression via FGF-8b to the upper jaw development of chick embryo, J Biosci Bioeng 119(3) (2015) 260-6.
[69] F.L.D. Tilton, J. K., Vue, M., Alzarban, N., Tanguay, R. L., Dithiocarbamates have a common toxic effect on zebrafish body axis formation, Toxicology and Applied Pharmacology 216(1) (2006) 55-68.
[70] J.E. Balmer, R. Blomhoff, Gene expression regulation by retinoic acid, Journal of Lipid Research 43 (2002) 1773-1808.
[71] B.L. Bohnsack, D. Gallina, H. Thompson, D.S. Kasprick, M.J. Lucarelli, G. Dootz, C. Nelson, I.M. McGonnell, A. Kahana, Development of extraocular muscles requires early signals from periocular neural crest and the developing eye, Arch Ophthalmol 129(8) (2011) 1030-41.
[72] C. Li, X. Shi, G. Zhou, X. Liu, S. Wu, J. Zhao, The canocical Wnt-beta-catenin pathway in development and chemotherapy of osteosarcoma, Frontiers in Bioscience (2013) 1384-1391.
[73] S. Herzig, S. Hedrick, I. Morantte, S.H. Koo, F. Galimi, M. Montminy, CREB controls hepatic lipid metabolism through nuclear hormone receptor PPAR-gamma, Nature 426(6963) (2003) 190-3.
[74] H.J. Heusinkveld, P.F. Wackers, W.G. Schoonen, L. van der Ven, J. Pennings, M. Luijten, Application of the comparison approach to open TG-GATEs: A useful toxicogenomics tool for detecting modes of action in chemical risk assessment, Food Chem Toxicol 121 (2018) 115-123.
[75] R.Y. Hampton, R.G. Gardner, J. Rine, Role of 26S proteasome and HRD genes in the degradation of 3-hydroxy-3-methylglutaryl-CoA reductase, an integral endoplasmic reticulum membrane protein., Molecular Biology of the Cell 7 (2017).
[76] Y. Ashikawa, Y. Nishimura, S. Okabe, S. Sasagawa, S. Murakami, M. Yuge, K. Kawaguchi, R. Kawase, T. Tanaka, Activation of Sterol Regulatory Element Binding Factors by Fenofibrate and Gemfibrozil Stimulates Myelination in Zebrafish, Frontiers in Pharmacology (2016).
[77] X. Hu, Gao, J., Liao, Y., Tang, S., lu, F., Retinoic acid alters the proliferation and survivalof the epithelium and mesenchyme and suppressesWnt/b-catenin signaling in developing cleft palate, Cell Death and Disease (4) (2013).
[78] E.B. Menegola, M<. L. Di Renzo, F., Giavini, E., Postulated pathogenic pathway in triazole fungicide induced dysmorphogenic effects, Reproductive Toxicology 22 (2006) 186-195.
[79] N. Funato, M. Nakamura, Identification of shared and unique gene families associated with oral clefts, Int J Oral Sci 9(2) (2017) 104-109.

[80] Q. Jiang, R.M. Lust, J.C. DeWitt, Perfluorooctanoic acid induced-developmental cardiotoxicity: are peroxisome proliferator activated receptor alpha (PPARalpha) and bone morphorgenic protein 2 (BMP2) pathways involved?, J Toxicol Environ Health A 76(11) (2013) 635-50.
[81] J.M. Iklé, A.L. Tavares, M. King, H. Ding, S. Colombo, B.A. Firulli, A.B. Firulli, K.L. Targoff, D. Yelon, D.E. Clouthier, Nkx2.5 regulates endothelin converting enzyme-1 during pharyngeal arch patterning, Genesis 55(3) (2017).
[82] C. Luckert, A. Braeuning , A. Lampen, L.T. Van der Ven, T. Bovee, Deliverable 3.1 - Development of CAG-specific PCR arrays, 2017.
[83] A.J. Williams, C.M. Grulke, J. Edwards, A.D. McEachran, K. Mansouri, N.C. Baker, G. Patlewicz, I. Shah, J.F. Wambaugh, R.S. Judson, A.M. Richard, The CompTox Chemistry Dashboard: a community data resource for environmental chemistry, Journal of Cheminformatics 9(1) (2017) 61.
[84] W. Slob, Dose-response modeling of continuous endpoints, Toxicological sciences : an official journal of the Society of Toxicology 66(2) (2002) 298-312.
[85] J.V. Cotterill, L. Palazzolo, C. Ridgway, N. Price, E. Rorije, A. Moretto, A. Peijnenburg, I. Eberini, Predicting estrogen receptor binding of chemicals using a suite of in silico methods - Complementary approaches of (Q)SAR, molecular docking and molecular dynamics, Toxicology and applied pharmacology 378 (2019) 114630.
[86] M. Rhinn, P. Dolle, Retinoic acid signalling during development, Development 139(5) (2012) 843-58.
[87] J.M. Gansner, B.A. Mendelsohn, K.A. Hultman, S.L. Johnson, J.D. Gitlin, Essential role of lysyl oxidases in notochord development, Developmental biology 307(2) (2007) 202-13.
[88] A.L. van Boxtel, J.M. Gansner, H.W. Hakvoort, H. Snell, J. Legler, J.D. Gitlin, Lysyl oxidase-like 3b is critical for cartilage maturation during zebrafish craniofacial development, Matrix biology : journal of the International Society for Matrix Biology 30(3) (2011) 178-87.
[89] J. Zhang, R. Yang, Z. Liu, C. Hou, W. Zong, A. Zhang, X. Sun, J. Gao, Loss of lysyl oxidase-like 3 causes cleft palate and spinal deformity in mice, Hum Mol Genet 24(21) (2015) 6174-85.
[90] H. Saito, J. Papaconstantinou, H. Sato, S. Goldstein, Regulation of a novel gene encoding a lysyl oxidase-related protein in cellular adhesion and senescence, J Biol Chem 272(13) (1997) 8157-60.
[91] A. Comptour, M. Rouzaire, C. Belville, N. Bonnin, E. Daniel, F. Chiambaretta, L. Blanchon, V. Sapin, Lysyl oxidase-like 4 involvement in retinoic acid epithelial wound healing, Scientific reports 6 (2016) 32688.
[92] R.G. Correa, V. Tergaonkar, J.K. Ng, I. Dubova, J.C. Izpisua-Belmonte, I.M. Verma, Characterization of NF-kappa B/I kappa B proteins in zebra fish and their involvement in notochord development, Mol Cell Biol 24(12) (2004) 5257-68.
[93] B. Cvek, Z. Dvorak, Targeting of nuclear factor-kappaB and proteasome by dithiocarbamate complexes with metals, Curr Pharm Des 13(30) (2007) 3155-67.
[94] F. Pietrocola, L. Galluzzi, J.M. Bravo-San Pedro, F. Madeo, G. Kroemer, Acetyl coenzyme A: a central metabolite and second messenger, Cell Metab 21(6) (2015) 805-21.
[95] M. Vogelauer, A.S. Krall, M.A. McBrian, J.Y. Li, S.K. Kurdistani, Stimulation of histone deacetylase activity by metabolites of intermediary metabolism, J Biol Chem 287(38) (2012) 32006-16.
[96] C.L. Galli, C. Sensi, A. Fumagalli, C. Parravicini, M. Marinovich, I. Eberini, A computational approach to evaluate the androgenic affinity of iprodione, procymidone, vinclozolin and their metabolites, PloS one 9(8) (2014) e104822.